

PAPER • OPEN ACCESS

## Pathway-specific cortico-muscular coherence in proximal-to-distal compensation during fine motor control of finger extension after stroke

To cite this article: Sa Zhou *et al* 2021 *J. Neural Eng.* **18** 056034

View the [article online](#) for updates and enhancements.

You may also like

- [Effects of a contusive spinal cord injury on cortically-evoked spinal spiking activity in rats](#)  
Jordan A Borrell, Dora Krizsan-Agbas, Randolph J Nudo et al.
- [Microspheres containing decellularized cartilage induce chondrogenesis \*in vitro\* and remain functional after incorporation within a poly\(caprolactone\) filament useful for fabricating a 3D scaffold](#)  
Paulomi Ghosh, Stacey M S Gruber, Chia-Ying Lin et al.
- [Smartphone-based remote assessment of upper extremity function for multiple sclerosis using the Draw a Shape Test](#)  
A P Creagh, C Simillion, A Scotland et al.




## PAPER

## OPEN ACCESS

RECEIVED  
15 January 2021REVISED  
21 August 2021ACCEPTED FOR PUBLICATION  
24 August 2021PUBLISHED  
21 September 2021Original content from  
this work may be used  
under the terms of the  
[Creative Commons  
Attribution 4.0 licence](#).Any further distribution  
of this work must  
maintain attribution to  
the author(s) and the title  
of the work, journal  
citation and DOI.

## Pathway-specific cortico-muscular coherence in proximal-to-distal compensation during fine motor control of finger extension after stroke

Sa Zhou<sup>1,2</sup>, Ziqi Guo<sup>1,2</sup>, Kiufung Wong<sup>1,2</sup>, Hanlin Zhu<sup>1,2</sup>, Yanhuan Huang<sup>1,2</sup>, Xiaoling Hu<sup>1,2,3,\*</sup>   
and Yong-Ping Zheng<sup>1,2</sup><sup>1</sup> Department of Biomedical Engineering, The Hong Kong Polytechnic University, Hong Kong, People's Republic of China<sup>2</sup> University Research Facility in Behavioural and Systems Neuroscience (UBSN), The Hong Kong Polytechnic University, Hong Kong, People's Republic of China<sup>3</sup> The Hong Kong Polytechnic University Shenzhen Research Institute, Shenzhen, People's Republic of China

\* Author to whom any correspondence should be addressed.

E-mail: [xiaoling.hu@polyu.edu.hk](mailto:xiaoling.hu@polyu.edu.hk)**Keywords:** stroke, compensatory movements, fine motor control, finger extension, upper extremity, directed corticomuscular coherence**Abstract**

**Objective.** Proximal-to-distal compensation is commonly observed in the upper extremity (UE) after a stroke, mainly due to the impaired fine motor control in hand joints. However, little is known about its related neural reorganization. This study investigated the pathway-specific corticomuscular interaction in proximal-to-distal UE compensation during fine motor control of finger extension post-stroke by directed corticomuscular coherence (dCMC). **Approach.** We recruited 14 chronic stroke participants and 11 unimpaired controls. Electroencephalogram (EEG) from the sensorimotor area was concurrently recorded with electromyography (EMG) from extensor digitorum (ED), flexor digitorum (FD), triceps brachii (TRI) and biceps brachii (BIC) muscles in both sides of the stroke participants and in the dominant (right) side of the controls during the unilateral isometric finger extension at 20% maximal voluntary contractions. The dCMC was analyzed in descending (EEG → EMG) and ascending pathways (EMG → EEG) via the directed coherence. It was also analyzed in stable (segments with higher EMG stability) and less-stable periods (segments with lower EMG stability) subdivided from the whole movement period to investigate the fine motor control. Finally, the corticomuscular conduction time was estimated by dCMC phase delay. **Main results.** The affected limb had significantly lower descending dCMC in distal UE (ED and FD) than BIC ( $P < 0.05$ ). It showed the descending dominance (significantly higher descending dCMC than the ascending,  $P < 0.05$ ) in proximal UE (BIC and TRI) rather than the distal UE as in the controls. In the less-stable period, the affected limb had significantly lower EMG stability but higher ascending dCMC ( $P < 0.05$ ) in distal UE than the controls. Furthermore, significantly prolonged descending conduction time ( $\sim 38.8$  ms) was found in ED in the affected limb than the unaffected ( $\sim 26.94$  ms) and control limbs ( $\sim 25.74$  ms) ( $P < 0.05$ ). **Significance.** The proximal-to-distal UE compensation in fine motor control post-stroke exhibited altered descending dominance from the distal to proximal UE, increased ascending feedbacks from the distal UE for fine motor control, and prolonged descending conduction time in the agonist muscle.

**List of abbreviations**

UE	upper extremity	ED	extensor digitorum
dCMC	directed corticomuscular coherence	FD	flexor digitorum
EEG	electroencephalogram	TRI	triceps brachii
EMG	electromyography	BIC	biceps brachii
		APB	abductor pollicis brevis
		PMC	premotor cortex

TMS	transcranial magnetic stimulation
SEP	somatosensory evoked potential
PET	positron emission tomography
fMRI	functional magnetic resonance imaging
CMC	cortico-muscular coherence
ECR	extensor carpi radialis
SMA	somatosensory area
MMSE	Mini-Mental State Examination
FMA	Fugl-Meyer Assessment
SNR	signal-to-noise ratio
MCP	metacarpophalangeal
PIP	proximal interphalangeal
IIR	infinite impulse response
iMVC	isometric maximum voluntary contraction
ICA	independent component analysis
AR	autoregressive
ACF	autocorrelation function
PACF	partial autocorrelation function
ANOVA	analysis of variance
EF	effect size
SEM	standard error of mean
NMES	neuromuscular electrical stimulation

## 1. Introduction

Compensatory movements are progressively developed as new movement strategies to replace impaired joint activities post-stroke in order to maintain daily functions [1, 2]. It is directly associated with the muscle weakness, spasticity, and muscle discoordination post-stroke [3], contributing to the occurrence of gross movement patterns rather than more advanced fine movements with independent joint activities [4]. As the high prevalence of permanent motor disabilities in hand motor functions in stroke population (up to 85%) [5], compensatory movements are commonly observed in the UE and typically manifested as considerable involvements of the proximal limb in distal movements (i.e. proximal-to-distal UE compensation), e.g. the elbow and shoulder locked with finger and wrist movements [2, 6]. As a result of the typically more severe impairments in extensors than flexors in the UE, finger extension is one of the motor functions most likely to be impaired and is impeded by inappropriate flexor activation in UE compensatory movements post-stroke [7]. The proximal-to-distal UE compensation is because that the difficulty of fine motor control related to hand dexterity prominently contributes to a delayed and poorer motor recovery in distal UE than the proximal [1, 8]. On the other hand, the adaptive strategy related to compensatory movements is a dominant force in shaping the dynamic process of repairing and remodeling the residual neural circuits, i.e. the neuroplasticity post-stroke [9]. Although the compensation seems to be helpful in a short-term, it may exacerbate long-term deficiencies such as reduced range of motion, abnormal inter-joint motions and pain after stroke [2], leading to ‘learned nonuse’ and

limiting motor restoration [6]. As indicated by Dayan *et al*, the maladaptive neuroplasticity resulting from compensatory movements post-stroke has been misinterpreted as motor recovery, as their overlapped contributions to performance improvements in a task [10, 11]. In particular, the subtle forms of compensation owing to impaired fine motor control, such as the postural instability, have been going undetected in the absence of sensitive behavioral measures [1, 2]. For example, the traditional clinical assessments focus on task accomplishment without enough attention on how the task is performed [2]. However, how the compensatory movements interfere with the positive neuroplasticity remains unclear [1]. This is principally due to a lack of effective evaluation on the neural reorganization in relation to compensatory movements during fine motor control of finger extension post-stroke. Such an investigation would promote the rehabilitation strategy planning for guiding treatments, particularly for the rehabilitation therapies with limited long-term effectiveness due to the uncorrected maladaptive neuroplasticity [2, 4].

Neuroplasticity on motor functions post-stroke was reported to be a bidirectional alteration involving both the efferent (descending) and afferent (ascending) corticomuscular pathways [12, 13], because the voluntary limb execution depends on the integration of motor control and sensory feedbacks within the closed-loop central-and-peripheral neuromuscular system [14, 15]. Particularly, fine motor control requires precise coordination between multisensory and motor systems [16, 17]. Studies on neuroplasticity related to compensatory movements post-stroke have mainly focused on the peripheral [6] or central motor system [18] alone or the coherent neural activity between them [19, 20]. In the peripheral motor system, compensation was characterized by excessive muscular participation of the proximal UE in the distal movements [6, 19, 21]. In the central motor system, the cortical reorganization related to the proximal-to-distal UE compensation promoted the hyperexcitability of the unaffected hemisphere [19], due to the anatomical arrangement of bilateral corticospinal innervation to the proximal UE [22, 23]. This cortical reorganization could be also characterized by the reduced spatial resolution of cortical representation in muscular discoordination [20] and by disinhibition in some regions within the affected hemisphere, such as the ipsilesional PMC [11]. Some TMS studies have indicated that ipsilateral motor projections were enhanced after stroke due to the compensation from the proximal muscles in the paretic UE, limiting the distal UE recovery [18, 24]. Taken together, these findings indicated either cortical reorganization or muscle discoordination in compensatory movements post-stroke. However, little is known of the pathway-specific neuroplasticity, i.e. the descending

and ascending pathways, between the reorganized motor cortex and the coordinated muscles in compensatory movements, mainly due to a lack of evaluation on bidirectional corticomuscular interaction with respect to both the proximal and distal UE in voluntary movements of the distal UE. This also leads to a lack of knowledge on the fine motor control related neuroplasticity post-stroke, which highly relies on the ascending multisensory input to adjust the descending motor command [25]. Therefore, the post-stroke bidirectional corticomuscular interaction in proximal-to-distal compensation during the fine motor control of finger extension remains to be studied.

dCMC could measure the directional influence between cortical and muscular activities, typically captured by the EEG and EMG signals [26, 27]. It has been applied to demonstrate the pathway-specific (i.e. descending and ascending pathways) corticomuscular interaction in the closed-loop sensorimotor control process in unimpaired [17, 28, 29] and stroke subjects [30–32]. Although TMS and SEP have also been used to measure the respective efferent and afferent nerve conduction post-stroke, they could only capture the static properties of corticomuscular pathways in a passive stimulation mode during the resting-state [17]. It limited the investigation on the altered voluntary motor control after stroke. In contrast to the TMS and SEP, the dCMC employing EEG and EMG during voluntary motor execution can capture the dynamic functional projection of motor commands and sensory feedbacks [26, 27], making it possible to investigate the pathway-specific alteration in compensatory movements and fine motor control post-stroke. Furthermore, because of the higher temporal resolution of EEG and EMG compared to other imaging techniques, e.g. PET and fMRI [33, 34], they are more suitable to detect transient neural responses, e.g. the sensory responses with temporal adaptation [15, 16]. In previous dCMC studies, Mima *et al* and Witham *et al* investigated dCMC on hand muscles, e.g. APB, in the unimpaired subjects during isotonic contraction tasks [28, 29]. They found that the relative magnitude of descending and ascending dCMC (i.e. EEG  $\rightarrow$  EMG and EMG  $\rightarrow$  EEG), representing the information flow asymmetry, could be more sensitive than the CMC approach, particularly for detecting the altered afferent input or unstable descending control [35]. Peterson *et al* investigated the fine motor control-related dCMC in eight lower limb muscles during the balance maintaining of walking and standing in unimpaired participants. It demonstrated that the descending dCMC was significantly higher than the ascending during either walking or standing, and there was a significantly increased descending dCMC in left medial gastrocnemius for fine motor control of the balance-perturbed standing [17]. Meng *et al* investigated dCMC on the ECR during wrist extension after

stroke. It was found that the ascending influence from the periphery to the primary SMA (S1) facilitated precise movements, and that the supplementary SMA exerted direct descending influence on the spinal sensorimotor circuits [30]. In a study on subacute stroke, dCMC was investigated in the FD and BIC during hand grasping and elbow flexion, respectively [32]. It demonstrated a shifted dominant direction of dCMC to the ascending pathway on the agonist muscle post-stroke, with significantly higher ascending dCMC than the descending dCMC, in contrast to the descending dominance in unimpaired controls, suggesting that the relative contribution of descending and ascending dCMC was altered in relation to the impaired voluntary motor control post-stroke. Overall, these studies suggested that dCMC was applicable to detect the pathway-specific corticomuscular interaction in voluntary movements, even in fine motor control. However, previous studies revealed only the agonist muscle-related bidirectional corticomuscular interaction in the affected limb. Little has been done on the compensatory movements related bidirectional corticomuscular interaction, mainly due to a lack of dCMC detection in the antagonist or other coordinated muscles. Particularly, little was known on the neural reorganization in the impaired fine motor control post-stroke, mainly due to a lack of evaluation on dCMC patterns in the stabilization of peripheral movements, which requires a typical bidirectional process on both motor commands and multisensory inputs [12, 16]. Bridging these knowledge gaps could provide a potential measure on the compensatory movements and the impaired fine motor control for clinical assessments, thereby guiding the rehabilitation strategy planning to correct the maladaptive neuroplasticity for long-term recovery [2, 4]. Therefore, the purpose of this study was to investigate the pathway-specific corticomuscular interaction on the proximal-to-distal UE compensation during the fine motor control of finger extension post-stroke, through the dCMC analyses on the four UE muscles, i.e. ED, FD, BIC and TRI.

## 2. Method

In this work, the pathway-specific corticomuscular interaction on compensatory movements in the fine motor control of finger extension post-stroke was investigated through the dCMC analysis between the sensorimotor cortex and the proximal and distal UE muscles. First, the steady-state isometric finger extension was conducted at both sides of the stroke subjects and at the dominant side of the unimpaired controls with synchronized EEG and EMG recordings. The dCMC strength was then analyzed in both descending (EEG  $\rightarrow$  EMG) and ascending pathways (EMG  $\rightarrow$  EEG) via the directed coherence. Furthermore, the EEG and EMG signals were subdivided into less-stable and stable periods based on the EMG

stability, to analyze the fine motor control-related pathway-specific CMC. Finally, the conduction time in descending and ascending pathways was estimated through the linear regression on the phase-frequency relationship of dCMC.

### 2.1. Subject recruitment

This study was approved by the Human Subjects Ethics Subcommittee of The Hong Kong Polytechnic University (approval number: HSEARS20170502002; HSEARS20190119001). The stroke subjects recruited in this study satisfied the following inclusion criteria, (a) 50–70 years old, (b)  $\geq 1$  year after the onset of unilateral brain lesions due to subcortical stroke, without other neurological impairments or secondary onset [36], (c) no visual, cognitive or attentional deficits (MMSE score  $> 21$ ) to ensure that the subject can understand and follow instructions during the experiment [37], (d) moderate to severe motor impairments on unilateral UE ( $15 < \text{FMA for UE (FMA-UE) score} < 45$ , with a maximal score of 66) [38], (e) modified Ashworth scale  $< 3$  for muscle tone at the elbow, wrist and fingers [39], (f) detectable voluntary EMG (i.e. triple the standard deviation (SD) above the baseline with an SNR  $> 50$  dB) from the UE muscles, ED, FD, TRI and BIC in the affected limb [21], (g) right-handed before the stroke onset. For unimpaired subjects, the inclusion criterion was 50–70 years old, and the corresponding exclusion criteria were (a) neurological deficits, (b) osteoarticular or peripheral neuromuscular disease in the UE, (c) left handedness, (d) current pregnancy, and (e) severe dysphasia or hypertension. Additionally, there was no specific requirement on the gender in subject recruitment, as the CMC was independent of the gender factor [29]. Finally, we recruited 14 stroke subjects and 11 age-matched ( $P > 0.05$ , independent  $t$ -test) unimpaired subjects as the control group (demographic data and clinical scores are presented in tables 1(a) and (b), respectively). In this work, only the dominant (right) limb of the unimpaired controls was used as the control limb to be compared with both sides of the stroke subjects. This was because that the unaffected side in either left or right hemiplegia could be considered as the dominant side, given the habitual adaptation in daily life at the very chronic stage post-stroke ( $\geq 10$  years, table 1(a)) [16]. Meanwhile, equal numbers of left and right hemiplegia (7/7, table 1(a)) were recruited to minimize possible dCMC differences between them, as practiced previously [16, 19]. All participants were informed of the research purpose and provided their written consents. The experiments were in accordance with the Declaration of Helsinki and local statutory requirements.

### 2.2. Experimental setup and protocol

The participant was invited to sit comfortably in front of the computer screen in a quiet and electromagnetic shielded laboratory. The testing forearm was placed

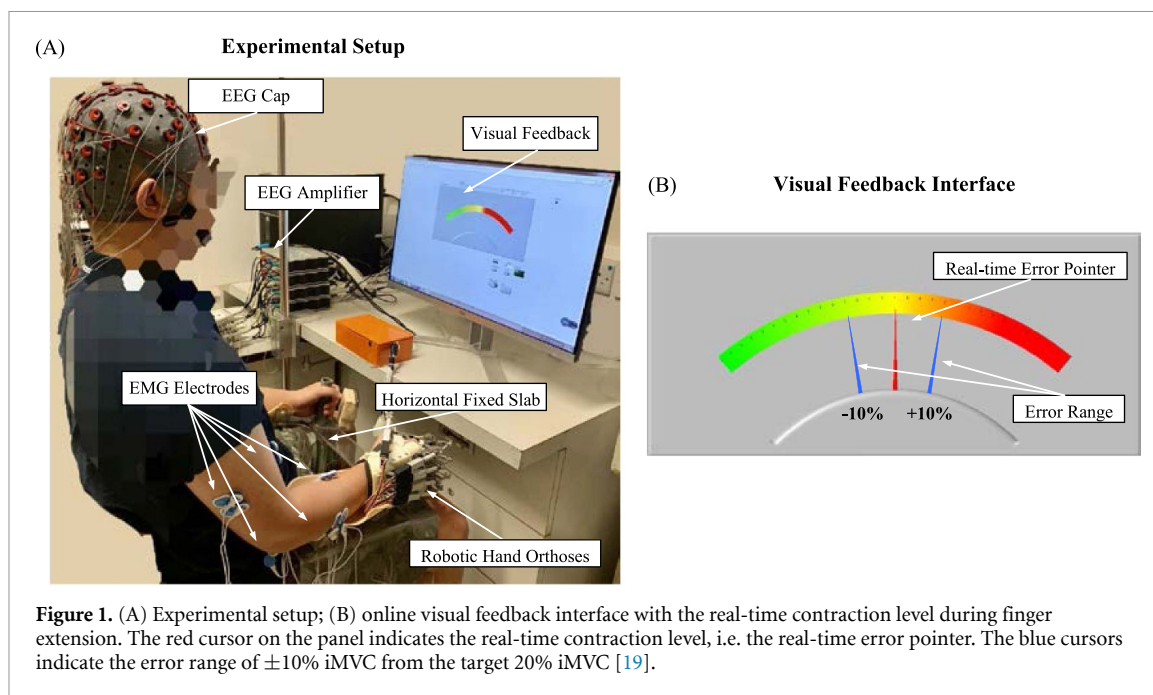
on a horizontal fixed slab in neutral position (figure 1(A)). The hand posture was standardized to make the force output plane orthogonal to the gravity. A 50% opened robotic hand orthosis with a palm-wrist module and five individual finger assemblies was then worn onto the hand to fix the wrist straight at  $0^\circ$ , the thumb at  $180^\circ$  at the MCP joint and  $165^\circ$  at the PIP joint, and the other four fingers at  $135^\circ$  at the MCP and  $135^\circ$  at the PIP joint [19]. A 64-channel EEG cap (g.GAMMASys active electrode system, g.tec medical engineering GmbH.) was used to record the 21-channel EEG signal from the sensorimotor cortex (i.e. CZ, CPZ, FCZ, C1-6, CP1-6, and FC1-6). The four-channel EMG electrodes (Blue SensorN, Ambu Inc.) were attached to the muscle belly of antagonist muscle pairs for the finger extension and flexion (ED and FD) and for the elbow extension and flexion (TRI and BIC) with a reference EMG electrode attached to the surface of the olecranon (figure 1(A)). The impedance of all EEG and EMG electrodes was prepared below  $5 \text{ k}\Omega$ . For the acquisition parameters, all EEG and EMG signals were synchronously recorded at a sampling rate of 1200 Hz, amplified with a gain of 10 000 for EEG (Amplifier: g.USBamp, g.tec medical engineering GmbH.) and 1000 for EMG (Amplifier: INA 333, Texas Instruments Inc.; DAQ: 6218 NI DAQ card, National Instruments Corp.). The signals were notch filtered at 50 Hz and band-pass filtered (EEG: 2–100 Hz; EMG: 10–250 Hz) in online processing for real-time display. All the filters in this work were the fourth order Butterworth IIR filter. The raw data were stored for offline processing. For online feedback of motion control (figure 1(B)), a self-programmed visual interface (LABVIEW 2015, National Instruments Corp.) was used to display the real-time contraction level (i.e. the red cursor) and the target range of 10%–30% iMVC (i.e. the blue cursors), according to the normalized EMG amplitude. The acquisition setup and visual feedback interface were detailed previously [19].

At the beginning of the experiment, the participants were instructed to perform the iMVC test as follows, (a) keep the testing upper limb relaxed to obtain the baseline EMG, (b) execute the iMVC of finger extension and flexion to obtain the maximum EMG on the respective ED and FD with the configuration in figure 1(A), (c) execute the iMVC of elbow extension and flexion to obtain the maximum EMG on the respective TRI and BIC, with the shoulder abducted at  $70^\circ$  and the elbow flexed at  $90^\circ$  [19]. Each iMVC was performed for 5 s and repeated thrice, with a 5 min break between two consecutive iMVCs to avoid muscle fatigue. The  $\text{EMG}_{\text{base}}$  and  $\text{EMG}_{\text{max}}$  in each muscle, representing the respective 0% iMVC and 100% iMVC, were calculated as the averaged EMG envelope (10 Hz low-pass filtering for the rectified EMG) over the respective baseline and iMVC tests [19]. The  $\text{EMG}_{\text{base}}$  and  $\text{EMG}_{\text{max}}$  from the ED were used to calculate the target range of 10%–30%

**Table 1.** (a) Demographic data of the recruited subjects. (b) Impairments measured by clinical scores in the recruited stroke subjects.

Group	No. of participants	Stroke types, hemorrhage/ ischemic	Affected side, left/right	Gender, male/female	Age (years, mean $\pm$ std)	Min/max years after stroke	(a)						
Stroke	14	7/7	7/7	3/11	56.5 $\pm$ 9.5	10/28							
Control	11	-/-	-/-	3/8	50.6 $\pm$ 16.8	-/-							
							(b)						
FMA full motor score							FMA	FMA wrist/hand	ARAT	FIM	MAS elbow	MAS wrist	MAS finger
Clinical assessment	44.38 $\pm$ 16.70	FMA shoulder/elbow	29.55 $\pm$ 9.60	14.95 $\pm$ 7.28	29.28 $\pm$ 18.35	65.43 $\pm$ 1.98	1.12 $\pm$ 0.56	0.87 $\pm$ 0.64	0.79 $\pm$ 0.51				

FMA, Fugl-Meyer Assessment [38]; FIM, functional independence measurement [78]; MAS, modified Ashworth score [39]; ARAT, Action Research Arm Test [79].



iMVC and the panel range of 0%–40% iMVC (i.e. the color gradient) (figure 1(B)). Next, the participant conducted the finger extension at 20% iMVC for 35 s with the limb position in (figure 1(A)). The finger extension was adopted because the extensor impairment was typically more severe than flexors in the UE after stroke [7]. The contraction level of 20% iMVC was selected because a constant and moderate contraction (<50% iMVC) can evoke evident CMC in the beta band (13–35 Hz) and avoid muscle fatigue compared to the higher levels, and was achievable for stroke persons [19, 40]. Another reason was that fine motor control was more related to lower-level contractions than higher-level contractions, due to more required efforts and cognitive concentration in lower force output [25, 41]. During the task, the subject was asked to maintain the red cursor at the mid-line of the panel (i.e. 0% deviation from the target 20% iMVC), with an allowable fluctuation within the two fixed blue cursors representing the target range of 10%–30% iMVC (figure 1(B)). A motion initiation period of 3 s was used to ensure that the subject reached the target range before the 35 s maintaining period. Each subject was required to perform five trials with a 2 min intertrial rest to avoid muscle fatigue. EEG and EMG signals were simultaneously recorded during the 35 s maintaining period. The subject was asked to minimize body movements, eye blinking and biting, and to avoid falling asleep or performing active mental tasks when conducting the target movement. Muscle fatigue was checked immediately after each trial according to the EMG mean power frequency (MPF) [19]. The same experimental protocol was applied for both sides in the stroke group and for the dominant (right) side in the control group.

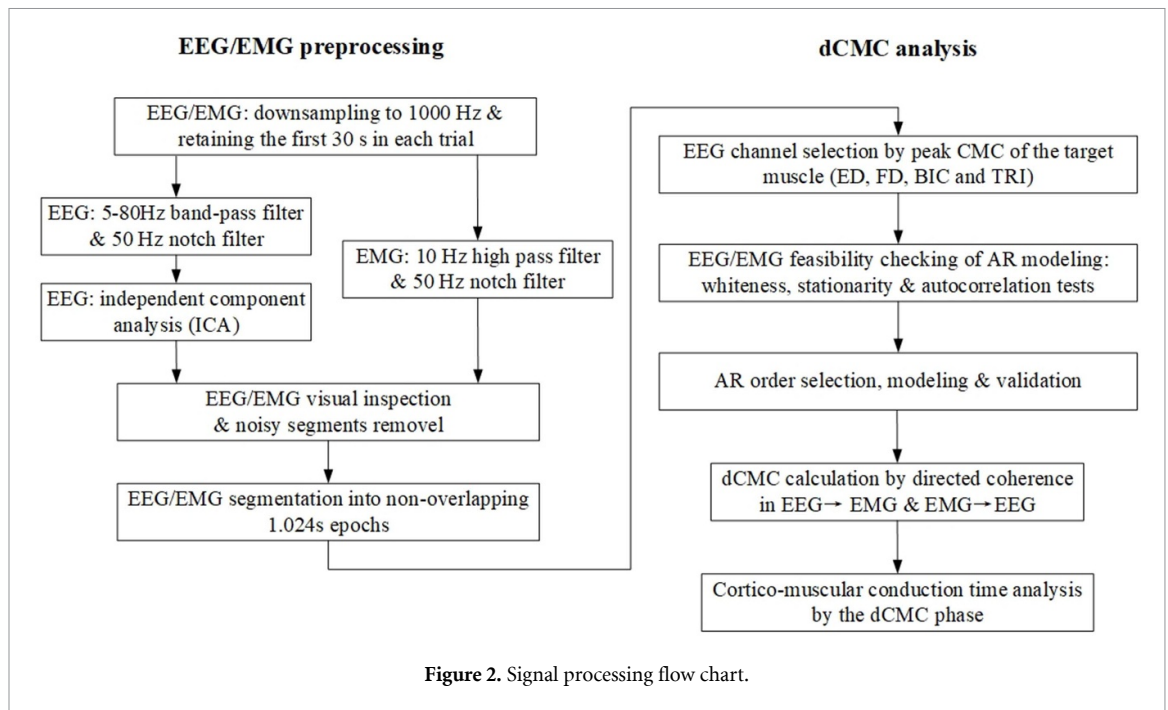
## 2.3. EEG and EMG processing

### 2.3.1. Data preparation

Figure 2 presents the procedures of the offline EEG/EMG processing in this work, which followed the general procedures in Fieldtrip and EEGLAB toolboxes and fulfilled the latest technique updates [42, 43]. The recorded raw EEG and EMG data were down-sampled to 1000 Hz; the first 30 s of the recorded EEG and EMG were retained by discarding the last 5 s in each trial to uniform the signal length and ensure the stability. Next, EEG signals were band-pass filtered to 5–80 Hz, notch filtered at 50 Hz and deparuted using ICA [44], to remove artifacts related to possible ocular movements, baseline drafts, and the line noise. EMG signals were filtered with a 10 Hz high-pass filter and notch filtered at 50 Hz. A visual inspection was undertaken for the EEG and EMG signals to reject any segments or channels with large motion artifacts. The power spectra of the EEG and EMG were plotted to confirm the signal quality for subsequent analyses, by checking additional environmental noises, e.g. harmonics of the line noise, and the power distribution, i.e. the decreased beta-band EEG power and the decreased EMG power on the agonist ED in the affected side after stroke [19, 45]. Afterwards, the EEG and EMG signals were segmented into nonoverlapping epochs with a unit length of 1024 point/epoch, as practiced previously [46].

### 2.3.2. EEG channel selection by peak CMC

The peak CMC in the beta band (13–35 Hz), indicating the ‘hot spot’ cortical area of the highest significant coherence with respect to the effector muscle [28, 46], was utilized to identify the EEG channel of interest from 21 channels in the sensorimotor area (i.e. CZ, CPZ, FCZ, C1-6, CP1-6, and FC1-6) with



respect to a target muscle (ED, FD, TRI, or BIC) in each participant. The CMC was calculated as the correlation between the EEG and EMG signals in the frequency domain, based on the classical definition of EEG-EMG coherence [19]. The CMC above the confidence level  $CL_{(\alpha\%)} = 1 - P^{N-1}$  in the beta band was considered to be significant, where  $CL_{(\alpha\%)} \in [0.0170, 0.0182]$  with a statistical significance level of  $P = 0.05$ , i.e.  $\alpha = 95$ , and the number of epochs  $N \in [164, 175]$ . The EEG channel with the highest significant CMC (i.e. the peak CMC) in the CMC topography was identified as the EEG channel of interest for the subsequent dCMC calculation [30].

### 2.3.3. dCMC analysis

The dCMC demonstrates the pathway-specific contribution to the neural interaction between the motor cortex and the effector muscles in finger extension. It was estimated using the directed coherence based on the AR modeling, also known as Granger causality [29, 47], between the EEG channel of interest, i.e. the EEG channel with peak CMC, and the EMG from a target muscle, i.e. ED, FD, TRI, or BIC, in each subject. The peak dCMC from the EEG to EMG in the beta band reflects the strength of descending motor control to the target muscle, whereas the reverse direction reflects the strength of ascending sensory feedback from the target muscle to the brain [29]. The dCMC is a model-based approach that the AR models the forward and backward interaction between EEG and EMG, and its bode diagram allows to investigate their frequency contents and phase shift (delay) knowing the residue  $E(t)$ . In this work, a bivariate AR model was fitted to the EEG  $X_{\text{EEG}}(t)$  and EMG  $X_{\text{EMG}}(t)$  signals, denoted as  $X(t) = (X_{\text{EEG}}(t), X_{\text{EMG}}(t))^T$ , from the respective

EEG channel of interest and the target muscle in each subject, according to the following equation [27, 28]:

$$\sum_{\tau=0}^k A(\tau)X(t-\tau) = E(t) \quad (1)$$

where  $E(t)$  is the residual vector of the white noise in each channel,  $A(\tau)$  is the  $2 \times 2$  matrix of model coefficients ( $A(0) = I$ , the identity matrix),  $\tau$  is the time delay, and  $k$  is the model order. A sufficiently high model order of  $k = 60$  was selected to achieve the necessary spectral resolution of 0.5 Hz and to adequately describe the conduction time between the EEG and EMG signals [30], where multiple information criteria were used for model order selection from 1 to 80, as practiced in [17]. In the AR modeling, the EEG and EMG signals were first normalized for a unit variance, then checked segment-by-segment to ensure its non-white noise, wide-sense stationary ( $|\lambda| < 1$  in the stability test, where  $\lambda$  is the eigenvalue of the AR model coefficient matrix) and be suitable to perform the AR modeling (trailed ACF and truncated PACF) [17]. The fitted AR model was validated for consistency, stability, and whiteness of residuals [48], to confirm that the autocorrelation structure of the signal was well captured by AR modeling. Meanwhile, the power spectra of the original EEG and EMG signals estimated using Welch's method were compared with those estimated from AR modeling to ensure the absence of spurious results ( $< \pm 1$  Hz deviation in the peak frequency) [30, 49].

The transfer function of the system  $H(f)$  and the residual  $E(f)$  were then obtained by z-transforming the AR model (equation (1)) into  $A(z)X(z) = E(z)$ , i.e.  $X(z) = A^{-1}(z)E(z) = H(z)E(z)$ , where



$z = e^{i2\pi f\Delta t}$  ( $i$  is the imaginary part,  $f$  is the frequency point and  $\Delta t$  is the time resolution) [27, 28]. Based on the  $H(f)$  and the covariance matrix  $C$  of the residual vector  $E(f)$ , the dCMC from EMG to EEG was calculated as follows [47]:

$$\text{dCMC}_{\text{EEG} \leftarrow \text{EMG}}(f) = \frac{|H_{12}(f)H_{12}^*(f)C_{22}|}{|H_{12}(f)H_{12}^*(f)C_{22} + H_{11}(f)H_{11}^*(f)C_{11}|} \quad (2)$$

where  $H_{12}(f)$  is the element in row 1 and column 2 in  $H(f)$ , representing the directional information transfer from EMG to EEG.  $H_{11}^*(f)$  represents the directional influence of the EEG on itself and “\*” denotes the complex conjugation.  $C_{11}$  and  $C_{22}$  are the elements in the covariance matrix  $C$  representing the respective noise contribution to the EEG and EMG. The significant level of dCMC was determined using a nonparametric statistical test based on the surrogate data with a significant level of  $P < 0.05$  [17, 29], where the surrogate data were obtained by randomly shuffling the phase structure of the original EEG and EMG signals with 1000 repetitions to minimize false positive results [50]. The non-significant dCMC with a peak value lower than the significant level was set to 0 for subsequent statistical comparisons [50]. Using the peak dCMC rather than the maximal value within the beta band to be compared with the significant level was because that the less-steady isometric contraction after stroke could lead to a shifted peak CMC to the gamma band with a still significant beta-band maximal value, which was observed previously in the dynamic contraction in unimpaired persons [51]. Similar directed coherence and its extensions were adopted previously to investigate dCMC and the cortico-cortical connectivity on sensory and motor functions in both stroke and unimpaired subjects [17, 31, 50].

The pathway-specific conduction time between the motor cortex and effector muscles was analyzed in each subject according to the phase-frequency relationship of the dCMC [29]. The phase information from EMG to EEG was obtained from the following equation:

$$\theta_{\text{EEG} \leftarrow \text{EMG}}(f) = \arg(H_{12}(f)) \quad (3)$$

where the  $\arg()$  represents taken the argument of the complex number, and  $H_{12}(f)$  is the element in the  $H(f)$  as in equation (2). The conduction time from EMG to EEG,  $T_{\text{EEG} \leftarrow \text{EMG}}$ , was then obtained from the respective phase delay in the beta band as  $T_{\text{EEG} \leftarrow \text{EMG}} = \Delta\theta_{\text{EEG} \leftarrow \text{EMG}}(f)/2\pi\Delta f$  [29]. It was calculated as the slope of the phase-frequency plot of  $\theta_{\text{EEG} \leftarrow \text{EMG}}(f)$  in the beta band using the linear fitting method [29]. The conduction time from EEG to EMG  $T_{\text{EMG} \leftarrow \text{EEG}}$  was calculated using the same procedure.

## 2.4. dCMC analysis in fine motor control

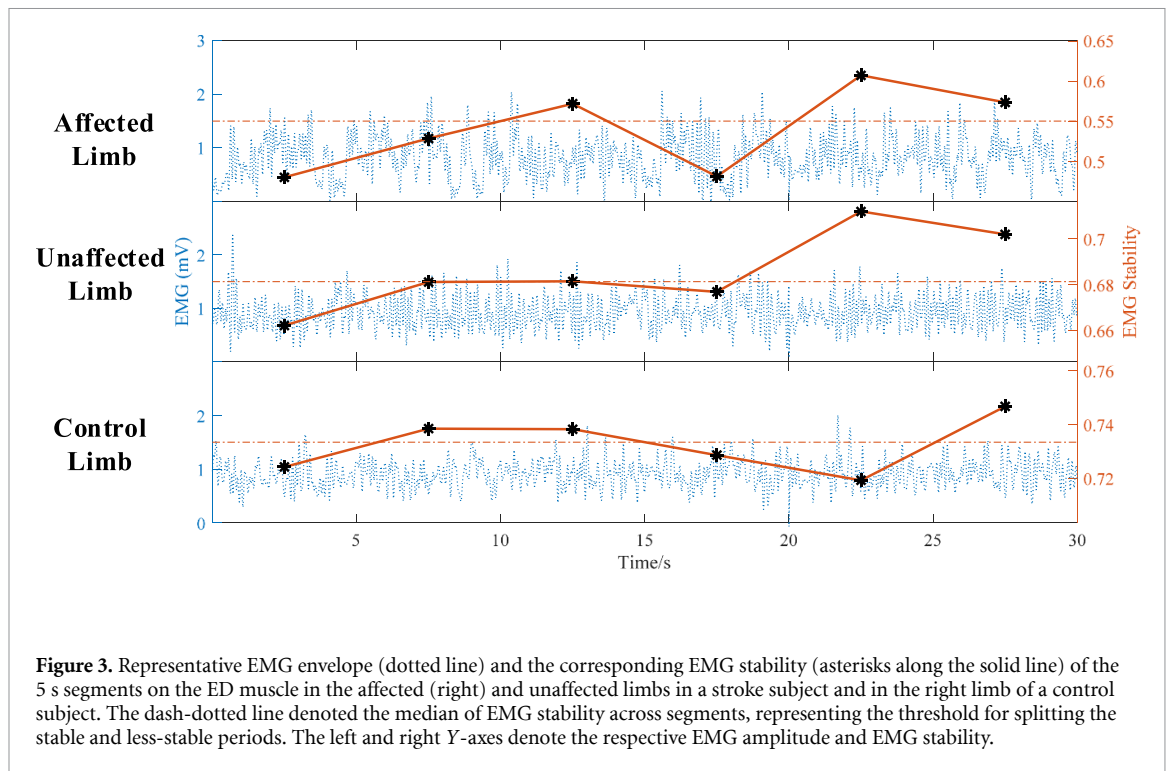
For the fine motor control-related pathway-specific CMC in compensatory movements, the dCMC pattern was further investigated in the less-stable period of sustained muscle contractions, in comparison with the stable period [1, 4]. The synchronous EEG and EMG signals in each trial were segmented and grouped into two contrasting periods, i.e. the stable and less-stable periods, using the median of EMG stability as the threshold, to capture the randomly presented less-stable EMG segments, as practiced in [52]. In figure 3, there was a randomness in the occurrence of the less-stable EMG segments over the 30 s finger extension (the asterisks below the dash-dotted line). It was related to the poor fine motor control in sustained isometric contractions at distal UE post-stroke, which was observed even in unimpaired subjects [52]. In this work, the whole data recorded over the five trials (the first 140 s was used for data length consistency) was divided into segments with a uniform length of 5 s [52], resulting in 28 segments for a muscle in each subject. The EMG stability was calculated for each segment as follows [52, 53]:

$$\text{EMG stability} = 1 - \frac{\text{SD}(\text{EMG}_{\text{envelope}})}{\text{Mean}(\text{EMG}_{\text{envelope}})} \quad (4)$$

where the EMG envelope was calculated as in section 2.2 and SD indicates the standard deviation. According to the median of EMG stability in each trial, the segments were then grouped into two periods, i.e. the stable period containing 14 segments with higher EMG stability and the less-stable period containing another 14 segments with lower EMG stability. Afterwards, the dCMC was calculated over each segment following the procedures mentioned in section 2.3.3, and then averaged across the segments in the respective stable and less-stable periods, generating two pairs of dCMC values to investigate the pathway-specific CMC for the fine motor control of finger extension.

## 2.5. Statistical analysis

The stroke group was further divided into the stroke affected group and the stroke unaffected group corresponding to the data captured from the related limbs, as the strategy of movement control was not only severely affected in the affected limb but also altered in the unaffected limb post-stroke compared with the unimpaired controls [54, 55]. After the Shapiro–Wilk test of normality, all variables, i.e. the dCMC strength in each pathway, the conduction time in each pathway and the EMG stability, were confirmed to obey the normal distribution. To begin, the intragroup comparison on the dCMC was conducted to test three null hypotheses that,  $H_{01}$ : there was no effect of the pathway factor (descending and ascending pathways) on the means of dCMC,  $H_{02}$ : there was no effect of the muscle factor (ED, FD, BIC, and



TRI) on the means of dCMC, and  $H_{03}$ : the effect of the pathway factor on the means of dCMC did not depend on the effect of the muscle factor (i.e. no effect of the pathway  $\times$  muscle interaction). The three null hypotheses were tested using a two-way ANOVA in each group (i.e. the stroke affected group, the stroke unaffected group and the control group). Post hoc tests of the two-way ANOVA were performed using the paired  $t$ -test for the pathway factor, and the one-way ANOVA for the muscle factor with either the Bonferroni post hoc test (for equal variance) or the Dunnett's T3 post hoc test (for unequal variance) for multiple comparison correction [15, 56].

Then, the intergroup comparison on the dCMC strength was conducted to test the null hypothesis that there was no effect of the group factor (the stroke affected group, the stroke unaffected group and the control group) on the means of dCMC in the whole movement period. It was tested using the one-way ANOVA with either the Bonferroni (for equal variance) or the Dunnett's T3 post hoc test. In addition, the intergroup comparison was also conducted on the variables of EMG stability and the dCMC strength in the stable and less-stable periods, to test the null hypotheses that,  $H_{01}$ : there was no effect of the group factor on the means of EMG stability in the subdivided (stable/less-stable) period, and  $H_{02}$  there was no effect of the group factor on the means of dCMC strength in the subdivided period. It was tested using the same statistical method as the whole movement period.

Finally, the corticomuscular conduction time in each pathway was statistically compared to test three null hypotheses that,  $H_{01}$ : there was no effect of the

group factor on the means of the conduction time,  $H_{02}$ : there was no effect of the muscle factor on the means of the conduction time, and  $H_{03}$ : the effect of the group factor on the means of the conduction time did not depend on the effect of the muscle factor (i.e. no effect of group  $\times$  muscle interaction). The three null hypotheses were tested using the two-way ANOVA in each pathway. Post hoc tests of the two-way ANOVA were performed using the one-way ANOVA with either the Bonferroni (for equal variance) or Dunnett's T3 post hoc test to compare the respective conduction time on varying muscles and on varying groups. The level of the statistical significance was set at 0.05 in this study, which was also indicated at 0.01 and 0.001. All statistical calculations were performed using SPSS 24.0 (2016).

### 3. Results

The total sample size of the EEG and EMG signals was 7680 epochs for the control group (rejection ratio: 0.25%), 9520 epochs for the unaffected side of the stroke group (rejection ratio: 2.8%), and 9323 epochs for the affected side of the stroke group (rejection ratio: 4.7%) after the data preprocessing. The data length of EEG and EMG signals was 140–150 s, i.e. 164–175 epochs, in a subject. There was no muscle fatigue across trials, i.e. less than 10% MPF reduction, and no additional environmental noise in the EEG/EMG power spectra. The power distribution agreed with previous findings, i.e. the decreased beta-band EEG power and the decreased EMG power on the agonist ED after stroke [19, 45]. Figure 4 shows the power spectra of EEG (C3 for the affected limb

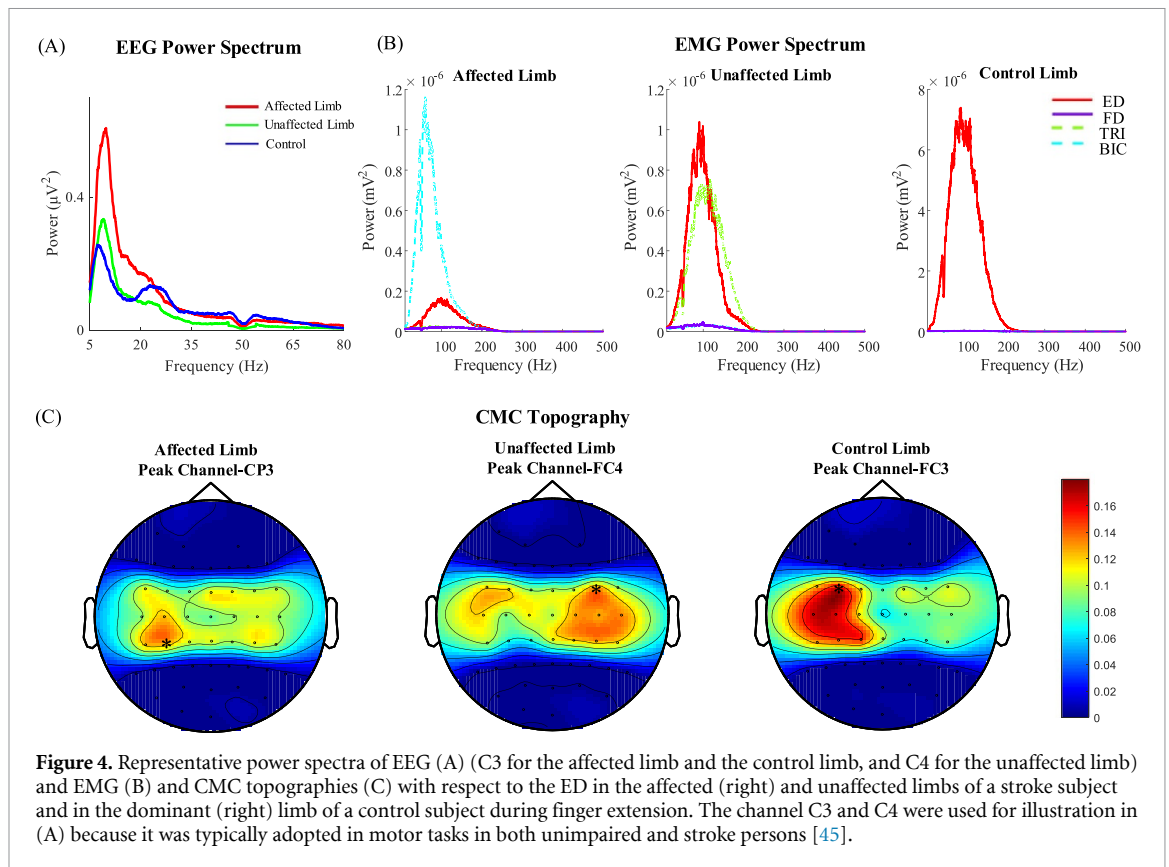


**Figure 4.** Representative power spectra of EEG (A) (C3 for the affected limb and the control limb, and C4 for the unaffected limb) and EMG (B) and CMC topographies (C) with respect to the ED in the affected (right) and unaffected limbs of a stroke subject and in the dominant (right) limb of a control subject during finger extension. The channel C3 and C4 were used for illustration in (A) because it was typically adopted in motor tasks in both unimpaired and stroke persons [45].

and the control, and C4 for the unaffected limb) and EMG and the CMC topographies with respect to ED in two representative subjects from the respective stroke and control groups during finger extension. In figure 4(A), there was a decreased beta-band EEG relative spectral power, i.e. the proportion of the beta-band (13–35 Hz) EEG power within the whole band of 5–80 Hz, in the affected limb compared to the unaffected and the control limbs. In figure 4(B), the EMG signal with the largest power was changed to the BIC in the affected limb after stroke, but it was found in ED in the unaffected and control limbs. In the CMC topographies (figure 4(C)), the EEG channel with the peak CMC, i.e. the EEG channel of interest for dCMC analysis, with respect to the ED was observed at ‘CP3’ in the affected limb, ‘FC4’ in the unaffected limb, and ‘FC3’ in the control limb, i.e. the contralateral sensorimotor area in each limb. This distribution was found in 64% (9/14) subjects in the stroke group and in 73% (8/11) subjects in the control group, which was detailed in the previous study [19].

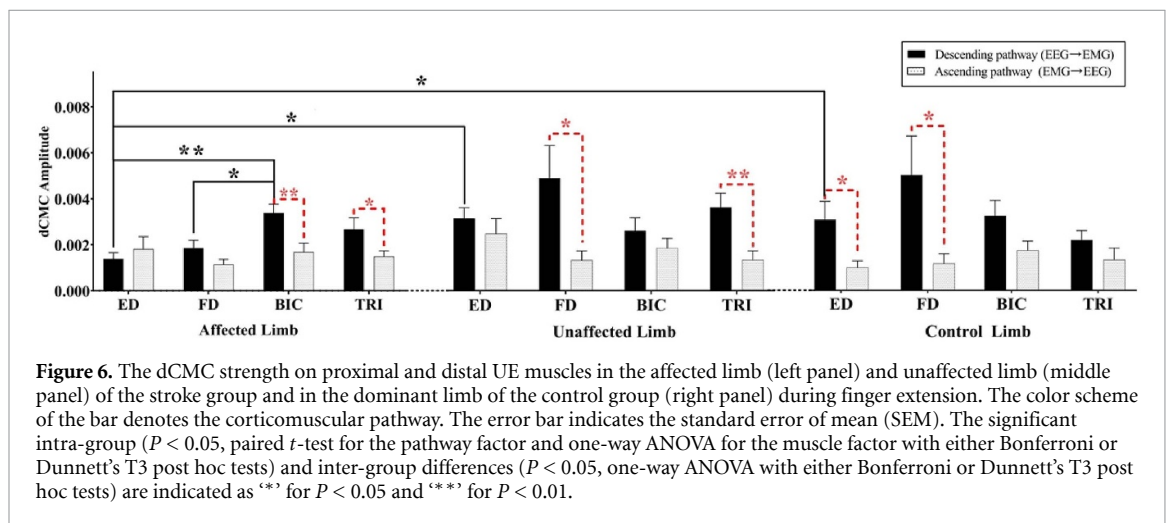
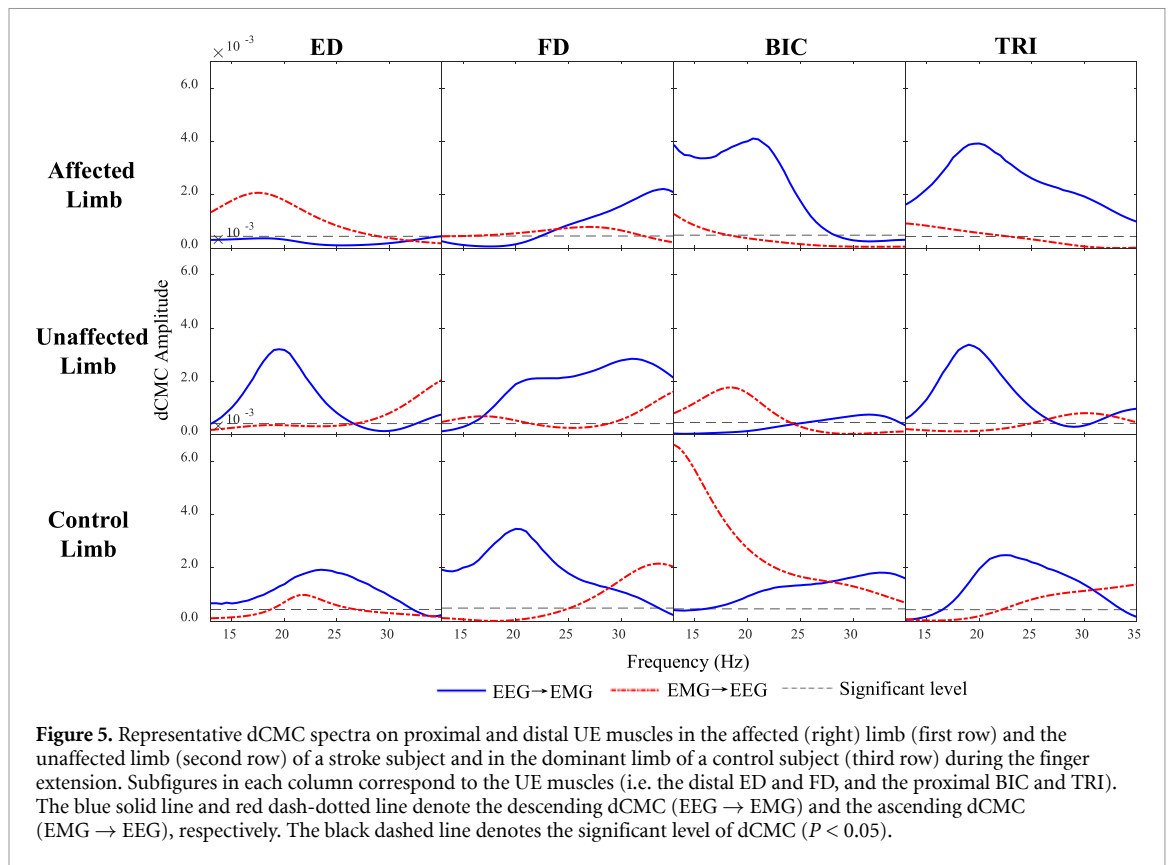
### 3.1. Representative dCMC spectra

Figure 5 shows the representative dCMC spectra on proximal and distal UE muscles in the affected and unaffected sides of a stroke subject and in the dominant side of a control subject during finger extension. In the affected limb, a significant dCMC peak in the descending pathway was observed in the FD, BIC and TRI rather than the ED. The significant ascending peak in the affected limb was observed in the distal

ED and FD with a higher value in ED than FD, but it was absent in the proximal BIC and TRI. The descending dominance (i.e. a higher dCMC peak in the descending pathway than the ascending pathway) did not show in the ED, rather showed in the FD, BIC and TRI in the affected limb during the finger extension. In the unaffected limb, the significant dCMC peak in the descending pathway was observed in all muscles, and the significant dCMC peak in the ascending pathway was observed in the FD, BIC and TRI. Although the ascending dCMC in ED in the unaffected limb had a significant maximal value at 35 Hz, no significant peak was observed within the beta band. The descending dominance in the unaffected limb was observed in the ED, FD and TRI, but was absent in the BIC. In the control limb, all muscles had the significant peaks in both descending and ascending pathways during finger extension (figure 5). Meanwhile, all muscles exhibited the descending dominance. In comparison with the unaffected and control limbs, the affected limb exhibited a distinct ascending dominance in the agonist ED and a prominent descending dominance in the proximal BIC and TRI and the antagonist FD.

### 3.2. Inter-group and intra-group comparisons on dCMC strength

Figure 6 shows the dCMC strength on proximal and distal UE muscles in both sides of the stroke group and in the dominant side of the control group during finger extension. Table 2 presents the two-way



ANOVA probabilities and the predicted EF represented by partial  $\eta^2$  with respect to factors of the muscle and the corticomuscular pathway in each UE group. Table 3 provides the detailed dCMC values presented as means and the 95% confidence intervals, in addition to the one-way ANOVA and paired  $t$ -test probabilities and estimated EFs. For the stroke affected limb (figure 6, left panel), there was a significantly higher dCMC in the descending pathway than the ascending ( $P < 0.01$ ,  $EF = 0.074$ , pathway main effect, two-way ANOVA, table 2) and a significant dCMC difference among ED, FD, BIC and TRI muscles ( $P < 0.05$ ,  $EF = 0.080$ , muscle main effect, two-way ANOVA, table 2). A significant interaction was also found

between the pathway and muscle factors ( $P < 0.05$ ,  $EF = 0.074$ , pathway  $\times$  muscle interaction, two-way ANOVA, table 2). The significantly higher dCMC in the descending pathway than the ascending, i.e. descending dominance, was found in the proximal UE, BIC and TRI ( $P < 0.05$ ,  $EF = 0.233$  in BIC and  $EF = 0.226$  in TRI, paired  $t$ -test, table 3), but not in the distal UE, ED and FD ( $P > 0.05$ ,  $EF = 0.1$  in ED and  $EF = 0.167$  in FD, paired  $t$ -test, table 3). Meanwhile, a significantly decreased descending dCMC was found in the distal muscles, ED and FD, than the proximal BIC ( $P < 0.01$ ,  $EF = 0.209$ , one-way ANOVA with the Bonferroni post hoc test  $P < 0.05$ , table 3).

**Table 2.** Comparisons on dCMC strength with respect to the factors of the muscle and pathway in each group.

Groups	Two-way ANOVA		
	Pathway P (partial $\eta^2$ )	Muscle P (partial $\eta^2$ )	Pathway $\times$ muscle P (partial $\eta^2$ )
Stroke group-affected limb	0.0034** (0.074)	0.0246* (0.080)	0.0349* (0.074)
Stroke group-unaffected limb	0.0004*** (0.146)	0.6097 (0.022)	0.1249 (0.069)
Control group	0.0003*** (0.152)	0.3455 (0.040)	0.2567 (0.049)

The superscript ‘\*\*’ indicates the significant main effect for the muscle and group factors or the significant interaction between the muscle and group factors (two-way ANOVA), with one superscript for  $P < 0.05$ , two superscripts for  $P < 0.01$ , and three superscripts for  $P < 0.001$ .

**Table 3.** dCMC strength with respect to the factors of the muscle and pathway in each group.

	Pathway Mean (95% confidence interval, E-03)	ED	FD	BIC	TRI	One-way ANOVA
		P (partial $\eta^2$ )				
Stroke group affected limb	Descending pathway (EEG $\rightarrow$ EMG)	1.39 (0.08–0.2)	1.86 (0.11–0.26)	3.39 (0.26–0.42)	2.54 (0.14–0.37)	0.0024** (0.209)
	Ascending pathway (EMG $\rightarrow$ EEG)	1.82 (0.07–0.3)	1.69 (0.09–0.25)	1.95 (0.08–0.31)	0.5924 (0.033)	
	Paired $t$ -test P (Cohen’s $d$ )	0.428 (0.100)	0.106 (0.167)	0.009** (0.233)	0.043* (0.226)	—
Stroke group unaffected limb	Descending pathway (EEG $\rightarrow$ EMG)	2.95 (0.2–0.39)	4.58 (0.16–0.76)	2.43 (0.12–0.36)	3.40 (0.21–0.47)	0.2857 (0.089)
	Ascending pathway (EMG $\rightarrow$ EEG)	2.31 (0.09–0.37)	1.73 (0.08–0.26)	1.26 (0.04–0.21)	0.3060 (0.085)	
	Paired $t$ -test P (Cohen’s $d$ )	0.413 (0.227)	0.041* (0.500)	0.383 (0.091)	0.009** (0.273)	—
Control group	Descending pathway (EEG $\rightarrow$ EMG)	2.85 (0.12–0.45)	4.65 (0.11–0.82)	3.00 (0.16–0.44)	2.03 (0.12–0.29)	0.2696 (0.092)
	Ascending pathway (EMG $\rightarrow$ EEG)	0.91 (0.03–0.15)	1.08 (0.02–0.2)	1.61 (0.08–0.24)	1.23 (0.02–0.23)	0.6208 (0.043)
	Paired $t$ -test P (Cohen’s $d$ )	0.024* (0.500)	0.033* (0.636)	0.053 (0.227)	0.315 (0.046)	—

The superscript ‘\*\*’ indicates the significant intra-group difference for the muscle factor (one-way ANOVA) and for the pathway factor (paired  $t$ -test), with one superscript for  $P < 0.05$  and two superscripts for  $P < 0.01$

For the stroke unaffected limb (figure 6, middle panel), there was also a significantly higher descending dCMC than the ascending dCMC ( $P < 0.001$ , EF = 0.146, pathway main effect, two-way ANOVA, table 2). Only the FD and TRI showed the descending dominance with a significantly higher dCMC in the descending pathway than the ascending ( $P < 0.05$ , EF = 0.5 in FD and EF = 0.273 in TRI, paired  $t$ -test, table 3). No significant dCMC difference was found among the UE muscles ( $P > 0.05$ , EF = 0.022, muscle main effect, two-way ANOVA, table 2). Meanwhile, no significant dCMC difference was found between the pathway and muscle factors ( $P > 0.05$ , EF = 0.069, pathway  $\times$  muscle interaction, two-way ANOVA, table 2).

For the control group (figure 6, right panel), the significantly higher descending dCMC than the

ascending dCMC was also observed ( $P < 0.001$ , EF = 0.152, pathway main effect, two-way ANOVA, table 2), as in the affected and unaffected limbs of the stroke group. The descending dominance with a significantly higher descending dCMC than the ascending was found in the distal UE, ED and FD ( $P < 0.05$ , EF = 0.5 in ED and EF = 0.636 in FD, paired  $t$ -test, table 3), but not in the proximal UE, BIC and TRI ( $P > 0.05$ , EF = 0.227 in BIC and EF = 0.046 in TRI, paired  $t$ -test, table 3). No significant dCMC difference was found among the UE muscles ( $P > 0.05$ , EF = 0.04, muscle main effect, two-way ANOVA, table 2). Meanwhile, no significant dCMC difference was found between the pathway and muscle factors ( $P > 0.05$ , EF = 0.049, pathway  $\times$  muscle interaction, two-way ANOVA, table 2).

**Table 4.** Intergroup comparisons on the dCMC strength with respect to the group factor for each pathway and each muscle.

Pathway	One-way ANOVA			
	ED P (partial $\eta^2$ )	FD P (partial $\eta^2$ )	BIC P (partial $\eta^2$ )	TRI P (partial $\eta^2$ )
Descending pathway (EEG $\rightarrow$ EMG)	0.037* (0.177)	0.111 (0.121)	0.400 (0.052)	0.204 (0.086)
Ascending pathway (EMG $\rightarrow$ EEG)	0.132 (0.092)	0.943 (0.003)	0.978 (0.001)	0.845 (0.041)

The superscript ‘\*’ denotes the significant inter-group difference with  $P < 0.05$  (one-way ANOVA).

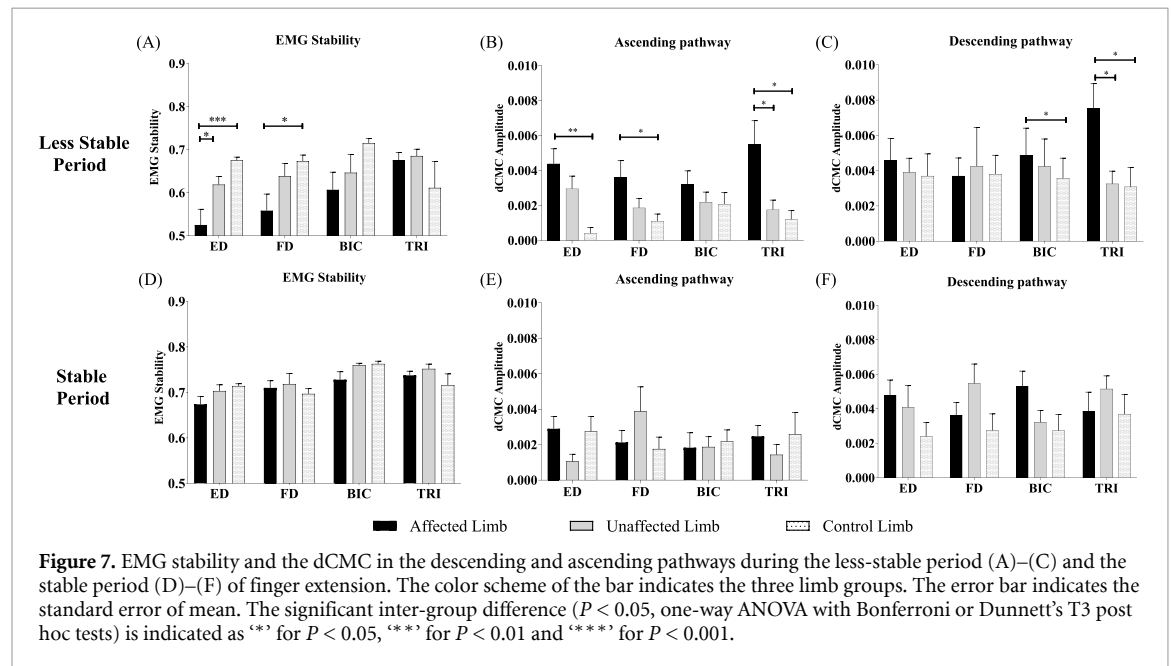


**Figure 7.** EMG stability and the dCMC in the descending and ascending pathways during the less-stable period (A)–(C) and the stable period (D)–(F) of finger extension. The color scheme of the bar indicates the three limb groups. The error bar indicates the standard error of mean. The significant inter-group difference ( $P < 0.05$ , one-way ANOVA with Bonferroni or Dunnett’s T3 post hoc tests) is indicated as ‘\*’ for  $P < 0.05$ , ‘\*\*’ for  $P < 0.01$  and ‘\*\*\*’ for  $P < 0.001$ .

In addition to the intra-group comparison, an inter-group comparison was also performed on the dCMC strength with respect to the UE group factor (i.e. the stroke-affected, stroke-unaffected and control group) in each muscle (figure 6). Table 4 presents the one-way ANOVA probabilities and predicted EFs represented by partial  $\eta^2$  with respect to the UE group factor in each corticomuscular pathway. In the descending pathway, the ED dCMC was significantly lower in the affected limb than the unaffected and the control limbs ( $P < 0.05$ , EF = 0.177, one-way ANOVA with the Dunnett’s T3 post hoc test  $P < 0.05$ , tables 3 and 4). Another distal muscle, FD, exhibited a decreasing trend in the mean values of descending dCMC in the affected limb compared with the unaffected and control limbs (figure 6), although it was not significant ( $P > 0.05$ , EF = 0.121, one-way ANOVA, table 4). The proximal muscles BIC and TRI also exhibited no significant difference on the descending dCMC among the UE groups ( $P > 0.05$ , EF = 0.052 in BIC and EF = 0.086 in TRI, one-way ANOVA, table 4). In the ascending pathway, no significant dCMC difference was observed in any muscle among the three UE groups ( $P > 0.05$ , one-way ANOVA, table 4).

### 3.3. dCMC in stable and less-stable periods

Figure 7 shows the EMG stability and dCMC during the less-stable period and the stable period of the finger extension task in the three UE groups. In the less-stable period (figures 7(A)–(C)), EMG stability in ED was observed to be significantly lower in the affected limb than the unaffected and control limbs ( $P < 0.001$ , EF = 0.338, one-way ANOVA with the Dunnett’s T3 post hoc test  $P < 0.05$ ) (figure 7(A)). The EMG stability in FD was also significantly lower in the affected limb than the control limb ( $P < 0.05$ , EF = 0.180, one-way ANOVA with the Dunnett’s T3 post hoc test  $P < 0.05$ ). No significant difference regarding the EMG stability was observed in the BIC and TRI among the three limb groups ( $P > 0.05$ , EF = 0.052 in BIC and EF = 0.088 in TRI, one-way ANOVA). In terms of the ascending dCMC (figure 7(B)), significantly higher values were observed in the ED and FD in the affected limb than the control limb ( $P < 0.05$ , EF = 0.292 in ED and EF = 0.203 in FD, one-way ANOVA with the Dunnett’s T3 post hoc test  $P < 0.05$ ). The TRI showed a significantly higher ascending dCMC in the affected limb than the unaffected and control limbs ( $P < 0.01$ , EF = 0.257, one-way ANOVA with the Dunnett’s

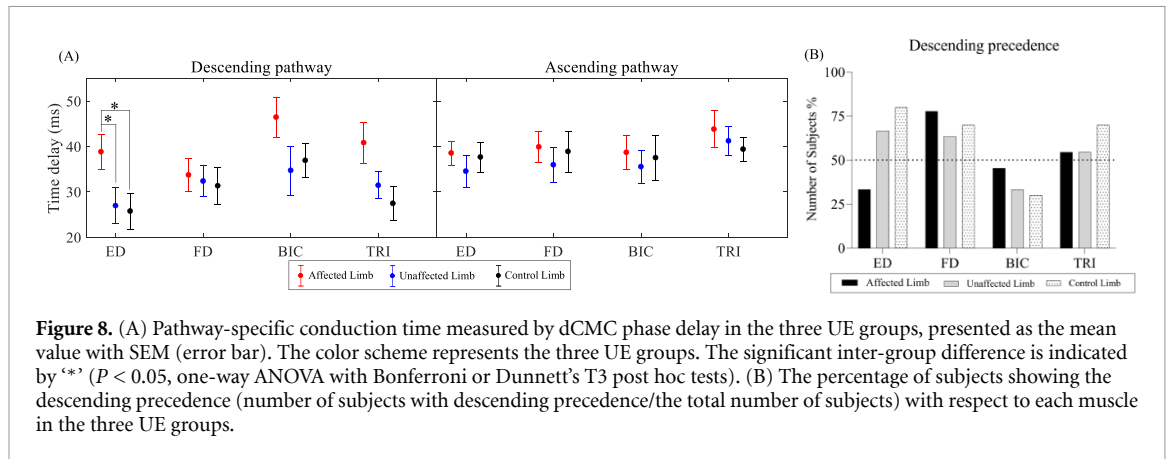


**Figure 8.** (A) Pathway-specific conduction time measured by dCMC phase delay in the three UE groups, presented as the mean value with SEM (error bar). The color scheme represents the three UE groups. The significant inter-group difference is indicated by '\*\*' ( $P < 0.05$ , one-way ANOVA with Bonferroni or Dunnett's T3 post hoc tests). (B) The percentage of subjects showing the descending precedence (number of subjects with descending precedence/the total number of subjects) with respect to each muscle in the three UE groups.

**Table 5.** Comparisons on the dCMC conduction time with respect to the factors of the group and the muscle.

Groups	Two-way ANOVA		
	Group P (partial $\eta^2$ )	Muscle P (partial $\eta^2$ )	Group $\times$ muscle P (partial $\eta^2$ )
Descending pathway	0.0012** (0.100)	0.0516 (0.059)	0.7317 (0.027)
Ascending pathway	0.4097 (0.014)	0.4123 (0.022)	0.9960 (0.005)

The superscript '\*\*' denotes the significant inter-group difference (two-way ANOVA) with two superscripts for  $P < 0.01$ .

T3 post hoc test  $P < 0.05$ ). No significant difference was found in the BIC regarding the ascending dCMC among the three limb groups ( $P > 0.05$ ,  $EF = 0.106$ , one-way ANOVA). In terms of the descending dCMC (figure 7(C)), the BIC showed a significantly higher value in the affected limb than the controls ( $P < 0.05$ ,  $EF = 0.172$ , one-way ANOVA with the Bonferroni post hoc test  $P < 0.05$ ). The TRI showed a significantly higher descending dCMC in the affected limb than the unaffected and control limbs ( $P < 0.05$ ,  $EF = 0.222$ , one-way ANOVA with the Bonferroni post hoc test  $P < 0.05$ ). No significant difference was found regarding the descending dCMC in distal muscles, ED and FD, among the three limb groups ( $P > 0.05$ ,  $EF = 0.051$  in ED and  $EF = 0.067$  in FD, one-way ANOVA). Unlike the less-stable period, there was no significant difference in the stable period regarding either EMG stability or dCMC strength in either pathways among the three limb groups ( $P > 0.05$ , one-way ANOVA, figures 7(D)–(F)).

### 3.4. dCMC phase delay

Figure 8(A) shows the pathway-specific conduction time measured by the dCMC phase delay in the three UE groups. Table 5 presents the two-way ANOVA probabilities and predicted EFs represented by partial  $\eta^2$  with respect to the UE group and muscle factors in each corticomuscular pathway. Table 6 provides detailed values of the conduction time presented as means and SEMs, in addition to the one-way ANOVA probabilities and the estimated EFs. For the

descending conduction time, there was a significant difference among the affected, unaffected and the control limbs ( $P < 0.01$ ,  $EF = 0.100$ , group main effect, two-way ANOVA, table 5). Further inter-group comparisons found a significantly prolonged descending conduction time in ED in the affected limb than the unaffected and control limbs ( $P < 0.05$ ,  $EF = 0.190$ , one-way ANOVA with the Bonferroni post hoc test  $P < 0.05$ , table 6, figure 8(A)). No statistical significance was observed among the ED, FD, BIC and TRI muscles ( $P > 0.05$ ,  $EF = 0.059$ , muscle main effect, two-way ANOVA, table 5), or between the group and muscle factors ( $P > 0.05$ ,  $EF = 0.027$ , group  $\times$  muscle interaction, two-way ANOVA, table 5). For the ascending conduction time, no significant difference was found with respect to different muscles, different UE groups or the interaction between the muscle and group factors ( $P > 0.05$ , group and muscle main effects and group  $\times$  muscle interaction, two-way ANOVA, table 5). Figure 8(B) shows the percentage of subjects with the descending precedence, i.e. time delay in the descending pathway  $<$  time delay in the ascending pathway, in each UE group. For the ED, only 34% stroke subjects showed the descending precedence in the affected limb, while 67% stroke subjects showed the descending precedence in the unaffected limb. By contrast, the control group had 80% subjects presenting the descending precedence in ED. The FD, BIC and TRI muscles showed relatively small differences ( $<20\%$ ) in the percentage of subjects with the descending precedence among the three UE groups.

**Table 6.** dCMC phase delay with respect to the factors of the group and muscle.

Variables		ED	FD	BIC	TRI	One-way ANOVA
		Mean $\pm$ SEM				P (partial $\eta^2$ )
Time delay in descending pathway (EEG $\rightarrow$ EMG)	Stroke group affected limb	38.81 $\pm$ 3.87	33.71 $\pm$ 3.69	46.45 $\pm$ 4.42	40.82 $\pm$ 4.52	0.197 (0.092)
	Stroke group unaffected limb	26.94 $\pm$ 3.93	32.36 $\pm$ 3.45	34.70 $\pm$ 5.40	31.42 $\pm$ 2.97	0.590 (0.046)
	Control group	25.74 $\pm$ 3.97	31.32 $\pm$ 4.11	36.91 $\pm$ 3.81	27.43 $\pm$ 3.66	0.199 (0.108)
	One-way ANOVA P (partial $\eta^2$ )	0.038* (0.190)	0.901 (0.007)	0.134 (0.108)	0.051 (0.169)	—
Time delay in ascending pathway (EMG $\rightarrow$ EEG)	Stroke group affected limb	38.53 $\pm$ 2.73	39.89 $\pm$ 3.31	38.67 $\pm$ 3.68	43.79 $\pm$ 4.10	0.684 (0.030)
	Stroke group unaffected limb	34.51 $\pm$ 3.44	35.95 $\pm$ 3.87	35.52 $\pm$ 3.68	41.21 $\pm$ 3.11	0.546 (0.051)
	Control group	37.65 $\pm$ 3.29	38.88 $\pm$ 4.53	37.51 $\pm$ 5.01	39.38 $\pm$ 2.62	0.984 (0.004)
	One-way ANOVA P (partial $\eta^2$ )	0.638 (0.028)	0.759 (0.017)	0.861 (0.009)	0.656 (0.026)	—

The superscript \* indicates the significant inter-group difference with  $P < 0.05$  (one-way ANOVA).

## 4. Discussion

In this work, we investigated the pathway-specific neuroplasticity post-stroke in proximal-to-distal UE compensation during fine motor control of finger extension, via dCMC analyses between the motor cortex and UE muscles (ED, FD, BIC and TRI). The results demonstrated that the proximal-to-distal UE compensation and impaired fine motor control were characterized by, (a) alteration in descending dominance from the distal to proximal UE, (b) increased ascending feedbacks from the distal UE for fine motor control, and (c) prolonged descending conduction time in the agonist ED.

### 4.1. Alteration of descending dominance after stroke

Intra-group and inter-group comparisons on the dCMC strength highlighted a reallocation of descending control from the distal to proximal muscles in the paretic UE during finger extension. The affected limb exhibited decreased descending control in the distal muscles and shifted descending dominance from the distal to proximal UE, in relation to compensatory movements. The results on dCMC strength showed that the descending dCMC of ED and FD was significantly lower than that of the BIC in the affected limb, and was significantly decreased (i.e. the ED) or had a decreased mean value (i.e. the FD) than the unaffected and control limbs (figure 6). The affected limb also showed a significantly higher descending dCMC than the ascending dCMC (i.e. descending dominance) in BIC and TRI, in contrast to the unimpaired group whose dCMC asymmetry was observed in ED and FD (figure 6). For the control group, the

consistent dCMC patterns with previous studies in the agonist muscle confirmed the effectiveness of the dCMC measurement in this work [17, 30, 32]. In this regard, similar findings on the descending dominance have been reported previously in the agonist muscle during isometric contractions, such as the ECR in wrist extension [30], the FD in finger flexion [32] and the leg muscles (e.g. tibialis anterior and medial gastrocnemius) in balance-perturbed walking and standing movements [17]. The descending and ascending pathways convey the respective sensations up to the brain and motor commands down to muscles via the efferent and afferent neurons in voluntary movements [13, 14, 57]. For the affected limb, the alterations observed in this work could be attributed to the maladaptive neuroplasticity in descending motor pathways in relation to the ‘learned disuse’ after stroke [11]. The descending control to the distal UE is primarily innervated by monosynaptic corticospinal pathways originating from the contralateral motor cortex, responsible for facilitating either flexors or extensors and inhibiting reciprocally for antagonism, in the unimpaired neuromuscular system [58, 59]. The significantly decreased descending control to the distal UE in this work was related to the denervated corticospinal tract with weakened monosynaptic connections following the brain lesions post-stroke [46, 60]. In addition, the alteration of descending dominance from the distal to proximal UE could be directly related to the altered cortical control to descending pathways, including the interhemispheric imbalance and competitive interaction in the affected hemisphere after stroke [11, 20]. In the interhemispheric imbalance, the abnormal coordination between the distal and proximal UE, e.g. the flexion



synergy in reaching tasks, was contributed by the increased ipsilateral motor projections to the paretic proximal UE in the hyperexcitability of the unaffected hemisphere post-stroke [61]. This ipsilateral cortical control to proximal UE was also found in isometric finger extension and flexion tasks post-stroke [19], given the anatomically bilateral corticospinal projections to the proximal UE [22]. Furthermore, the hand and proximal arm were reported to compete for expression within the motor cortex [20], in the weakened inhibition in the ipsilesional PMC [62]. Therefore, our findings regarding the shifted descending dominance from the distal to proximal UE suggested that the descending control was reallocated to the proximal muscles during finger extension in the paretic UE, mainly due to the compensation of the contralesional hemisphere and weakened inhibition in the ipsilesional PMC.

In addition to the affected UE, the alteration in descending dominance was also captured in the unaffected UE in this work (figure 6). The results showed that the unaffected UE had a descending dominance in FD and TRI, rather than in ED and FD as in the control group, although no significant difference was observed in either descending or ascending dCMC with respect to the control group. It suggested a shifted pattern of the descending dominance from the agonist ED to the synergistic extensor TRI in the unaffected limb post-stroke. This was because that the disinhibition of the primary motor cortex in the unaffected hemisphere contributed to an altered inhibition to proximal muscles in distal movements [63, 64]. In contrast to the extensively studied paretic side, studies on the less severely affected non-paretic side were conducted mainly in terms of the muscle kinematics or activation levels in the peripheral. For example, Nowak *et al* found that the dexterity represented by kinematic parameters was impaired for both proximal and distal segments in the unaffected UE during reaching and grasping post-stroke [54]. Bowden *et al* further demonstrated that voluntary activation of proximal muscles was weakened in the unaffected UE and was related to a functional alteration in the corticospinal drive to muscles rather than the anatomical factors [55]. Our results indicated that the functional alteration in the unaffected limb involved a shifted pattern of descending dominance from the agonist ED to the synergistic extensor TRI in finger extension.

#### 4.2. Increased ascending feedback for fine motor control after stroke

In the distal muscles, ED and FD, the increased ascending feedback was captured for fine motor control during the less-stable period of sustained finger extension at 20% iMVC. The results found that, in the less-stable period, the ED and FD in the affected limb had a significantly lower EMG stability and a significantly higher ascending dCMC without

significant change in the descending pathway compared with the controls (figure 7). The observed lower EMG stability suggested impaired fine motor ability in the distal UE after stroke, given the significant correlation between the precision of force production and EMG stability in steady-state isometric contractions as suggested previously in [25, 52]. Meanwhile, the unidirectional enhancement in the ascending corticomuscular pathway suggested that the impaired fine motor ability could be attributed to the impaired recalibration function responsible for stabilizing the peripheral state. For the sensorimotor recalibration in the unimpaired, the descending motor command was continuously modulated until a certain level by comparing the expected and actual levels of sensory reafference, e.g. proprioceptive information on the muscle length and joint position through spindle afferents, during the sustaining process of steady-state motor tasks [65, 66]. The findings of increased ascending dCMC in this work suggested that the descending motor command failed to respond to the afferent peripheral information on the muscle tension from Golgi tendon organs or muscle length variation from muscle spindles, resulting in a less-stable peripheral state. In studies on unimpaired persons, similar inverse relationships between corticomuscular interaction and fine motor performance have been found among different muscles [17, 25, 41]. For stroke participants, previous studies suggested that impaired recalibration function of the sensorimotor system contributed to the lower limb postural instability [13] and altered modulatory effects of sensory-level NMES [31]. For example, a similar unidirectional enhancement in the ascending pathway was found by Bao *et al* in stroke subjects during the sensory-level NMES-driven rhythmic pedaling, in contrast to the bidirectional enhancement of both pathways in the unimpaired [31]. In the present study, the results of EMG stability and dCMC in the distal UE demonstrated that the impaired fine motor control post-stroke could be characterized by the unidirectional enhancement in the ascending pathway, due to impaired recalibration function in the sensorimotor system.

Unlike the distal UE, the proximal UE in the less-stable period exhibited no significant difference in EMG stability in either BIC or TRI, a bidirectionally enhanced dCMC in TRI, and a unidirectionally enhanced descending dCMC in BIC in the affected limb compared with the unaffected and control limbs (figure 7). This suggested the relatively preserved functions of sensorimotor recalibration for correcting the unstable movement in the proximal UE, via the recruited ventromedial corticomuscular projections [61]. The results also indicated that the fine motor control in distal muscles could be restricted by the shifted pattern of descending control from the distal to proximal UE. For example, the enhancement of descending dCMC in the BIC could be resulted

from the flexion synergy between the UE flexors, e.g. the FD and BIC, which restricted elbow extension [1] and hand opening [67] and contributed to the gross movement pattern in the UE [61]. Therefore, the findings in the less-stable period suggested that the impaired fine motor control in the distal UE could also be resulted from the shifted descending control from the distal to proximal UE, due to the relatively preserved recalibration function in the proximal BIC and TRI.

#### 4.3. Prolonged conduction time in the descending pathway

For the control group, the comparable conduction time to those in the previous studies on the dCMC phase delay further confirmed the effectiveness of the dCMC in capturing the dynamic functional projection of motor command and sensory feedbacks in finger extension in the current study [29, 52]. The conduction time (figure 8, table 6) with respect to the agonist ED in the unaffected limb ( $\sim 26.94$  ms for the descending pathway and  $34.51$  ms for the ascending) and the control limb ( $\sim 25.74$  ms for the descending and  $\sim 37.65$  ms for the ascending) was in reasonable agreement with the previously suggested range of 20–40 ms in unimpaired individuals, such as the phase delay estimated by dCMC in finger muscles ( $\sim 26.4$  ms for the descending and  $\sim 29.5$  ms for the ascending) [52] and computational modeling in hand muscles (32 ms for the descending) [29].

For the distal UE in the affected limb, the descending conduction efficiency was found to have a significant reduction in the agonist ED and no significant change in the antagonist FD. The results showed that ED in the affected limb ( $\sim 38.8$  ms) had a significantly prolonged conduction time in the descending pathway and a markedly reduced percentage of subjects (46%) exhibiting the descending precedence, compared with the unaffected limb and the control group, whereas the FD showed no significant change regarding either the conduction time or the descending precedence among the three limb groups (figure 8, table 6). For the ED, similar findings on the decreased conduction efficiency in the agonist muscle have been reported previously in CMC [46] or TMS [60] studies on stroke persons. This was because that the reduction of available fast pyramidal tracts innervated by the affected hemisphere contributed to an insufficient discharge of motoneurons, according to the temporal summation mechanism at the spinal cord [68, 69]. For the antagonist FD, the unchanged conduction efficiency could be resulted from the long-term adaptation of the flexors to the frequent force production in activities of daily living and the reduced inhibition of upper motor neurons in weakened antagonism after stroke [41, 70, 71], despite the reduced corticospinal tracts and the decreased descending control as in the agonist ED. For example,

the weakened antagonism post-stroke was found in the failed inhibition of antagonist forearm muscles during the median nerve stimulation [71]. Therefore, the analyses on dCMC phase delay in this work suggested that the descending conduction efficiency was decreased in the agonist ED without significant change in the antagonist FD during finger extension post-stroke.

For the proximal UE, BIC and TRI, no significant difference was found either in the intergroup comparison among the three UE groups or in the intragroup comparison with respect to other UE muscles (figure 8, table 6). It suggested that the conduction time of the proximal UE was similar to that of the distal UE in both subject groups during finger extension. For the unaffected limb and the control group, this could be related to the very low contraction level of proximal muscles in finger extension, because that the central motor conduction time in active muscles was shorter than the resting muscles as suggested in TMS studies [72]. For the affected limb, although a shorter conduction time was expected to appear in the proximal than the distal UE due to the muscle contraction, the similar conduction time among proximal and distal UE muscles in this work could be attributed to the less-dense extrapyramidal tracts innervating the proximal muscles for compensation to distal movements, compared to the fast pyramidal tracts [73]. For example, the corticoreticular and reticulospinal pathways innervating the proximal flexor, e.g. BIC, in the ventromedial spinal cord contained fewer tract fibers (15% pyramidal tract fibers) than the dorsolateral corticospinal pathway (85% pyramidal tract fibers) responsible for skilled motor control [74]. Therefore, the dCMC phase delay of the BIC and TRI indicated that the proximal UE had a similar corticomuscular conduction time to the distal UE in the recruited corticomuscular pathways for compensatory movements, despite the shifted descending dominance from the distal to proximal muscles observed in this study.

One of the limitations in this work was the small sample size for chronic stroke, while the current results elucidated the characteristics of pathway-specific CMC on proximal-to-distal UE compensation during the fine motor control of finger extension after stroke. Although the left and right hemiplegia typically experienced the same treatments and their affected sides were compared with the unaffected sides or unimpaired controls [6, 16], previous studies also suggested that the stroke hemispheric lateralization could influence the motor performance and muscular synergies differently [75, 76]. Therefore, in the future work, we will increase the sample size of the stroke group to compare the difference of dCMC patterns between the left- and right-hemiplegia, as little was known on the effects of the lesion site on dCMC post-stroke. In addition, machine learning methods,

e.g. the support vector machine [77], will be used for classification on the dCMC features between the stroke and unimpaired persons during the fine motor control of finger extension, to demonstrate the utility of dCMC as a diagnostic biomarker on compensatory movements after stroke. Furthermore, regression analyses on the dCMC features, via the convolutional neural network [77], will be performed to predict the clinical scores at the pre-, post-intervention and follow-ups in rehabilitation programs, to provide insights on the clinical prognosis of compensatory movements and fine motor control.

## 5. Conclusion

In this work, we investigated the pathway-specific corticomuscular interactions in proximal-to-distal UE compensation during fine motor control of finger extension post-stroke, via dCMC analyses between the motor cortex and UE muscles (ED, FD, BIC and TRI). The results demonstrated that the proximal-to-distal UE compensation and the related fine motor control post-stroke were characterized by an alteration in descending dominance from the distal to proximal UE, increased ascending feedbacks from the distal UE for fine motor control in the less stable period, and prolonged descending conduction time in the agonist ED. Specifically, the altered descending dominance from the distal to proximal UE in the affected side was visualized by the significantly higher descending dCMC than the ascending in BIC and TRI, in contrast to the controls whose dCMC asymmetry was in ED and FD. This could also be reflected by the significantly lower descending dCMC of the ED and FD than the BIC in the affected limb, due to the compensation of the contralesional hemisphere and weakened inhibition in the ipsilesional PMC. For the pathway-specific CMC in fine motor control, increased ascending feedbacks from the distal UE were observed in the significantly increased ascending dCMC without significant alteration in the descending dCMC in the less-stable period. It was related to the weakened sensorimotor recalibration for fine motor control in the paretic distal joints and the shifted descending control to the proximal joints. Furthermore, the descending conduction time in the affected limb was prolonged in the ED without significant change in the proximal muscles, because of the discontinuity in corticospinal tracts innervating the agonist ED and the small number of extrapyramidal tracts innervating the proximal UE in compensatory movements.

## Data availability statement

The data generated and/or analyzed during the current study are not publicly available for legal/ethical reasons but are available from the corresponding author on reasonable request.

## Acknowledgments

The authors would like to thank the participants who participated in this study. This project was funded by National Natural Science Foundation of China (NSFC 81771959) and University Grants Committee Research Grants Council, Hong Kong (GRF 15207120).

## Ethical statement

The human experiments were conducted after we obtained the ethical approval from the Human Subjects Ethics Sub-Committee of The Hong Kong Polytechnic University (Approval Numbers HSEARS20170502002 and HSEARS20190119001) and the written informed consent from all subjects. All participants are aware of the intended publication. The experiments are in accordance with the Declaration of Helsinki and local statutory requirements.

## ORCID iD

Xiaoling Hu  <https://orcid.org/0000-0003-3188-3005>

## References

- [1] Jones T A 2017 Motor compensation and its effects on neural reorganization after stroke *Nat. Rev. Neurosci.* **18** 267–80
- [2] Levin M F, Kleim J A and Wolf S L 2009 What do motor ‘recovery’ and ‘compensation’ mean in patients following stroke? *Neurorehabil. Neural Repair* **23** 313–9
- [3] Dewald J P A, Pope P S, Given J D, Buchanan T S and Rymer W Z 1995 Abnormal muscle coactivation patterns during isometric torque generation at the elbow and shoulder in hemiparetic subjects *Brain* **118** 495–510
- [4] Cirstea M and Levin M F 2000 Compensatory strategies for reaching in stroke *Brain* **123** 940–53
- [5] Bailey R R, Klaesner J W and Lang C E 2015 Quantifying real-world upper-limb activity in nondisabled adults and adults with chronic stroke *Neurorehabil. Neural Repair* **29** 969–78
- [6] Qiuyang Q, Nam C, Guo Z, Huang Y, Hu X, Ng S C, Zheng Y and Poon W 2019 Distal versus proximal—an investigation on different supportive strategies by robots for upper limb rehabilitation after stroke: a randomized controlled trial *J. Neuroeng. Rehabil.* **16** 64
- [7] Kamper D, Harvey R L, Suresh S and Rymer W Z 2003 Relative contributions of neural mechanisms versus muscle mechanics in promoting finger extension deficits following stroke *Muscle Nerve* **28** 309–18
- [8] Roby-Brami A, Fuchs S, Mokhtari M and Bussel B 1997 Reaching and grasping strategies in hemiparetic patients *Motor Control* **1** 72–91
- [9] Jones T A, Allred R P, Jefferson S C, Kerr A L, Woodie D A, Cheng S-Y and Adkins D L 2013 Motor system plasticity in stroke models: intrinsically use-dependent, unreliably useful *Stroke* **44** S104–S6
- [10] Dayan E and Cohen L G 2011 Neuroplasticity subserving motor skill learning *Neuron* **72** 443–54
- [11] Takeuchi N and Izumi S-I 2012 Maladaptive plasticity for motor recovery after stroke: mechanisms and approaches *Neural Plast.* **2012** 359728
- [12] Campfens S F, Zandvliet S B, Meskers C J, Schouten A C, van Putten M J and van der Kooij H 2015 Poor motor function is

- associated with reduced sensory processing after stroke *Exp. Brain Res.* **233** 1339–49
- [13] Marigold D S, Eng J J, Tokuno C D and Donnelly C A 2004 Contribution of muscle strength and integration of afferent input to postural instability in persons with stroke *Neurorehabil. Neural Repair* **18** 222–9
- [14] Taube J S 2007 The head direction signal: origins and sensory-motor integration *Annu. Rev. Neurosci.* **30** 181–207
- [15] Huang Y, Jiao J, Hu J, Hsing C, Lai Z, Yang Y and Hu X 2020 Measurement of sensory deficiency in fine touch after stroke during textile fabric stimulation by electroencephalography (EEG) *J. Neural Eng.* **17** 045007
- [16] Zhou S, Huang Y, Jiao J, Hu J, Hsing C, Lai Z, Yang Y and Hu X 2021 Impairments of cortico-cortical connectivity in fine tactile sensation after stroke *J. Neuroeng. Rehabil.* **18** 34
- [17] Peterson S M and Ferris D P 2019 Group-level cortical and muscular connectivity during perturbations to walking and standing balance *NeuroImage* **198** 93–103
- [18] Chen R et al 2008 The clinical diagnostic utility of transcranial magnetic stimulation: report of an IFCN committee *Clin. Neurophysiol.* **119** 504–32
- [19] Guo Z, Qian Q, Wong K, Zhu H, Huang Y, Hu X and Zheng Y 2020 Altered corticomuscular coherence (CMCoh) pattern in the upper limb during finger movements after stroke *Front. Neurol.* **11** 410
- [20] Yao J and Dewald J P (ed) 2006 Cortico-muscular communication during the generation of static shoulder abduction torque in upper limb following stroke 2006 *Int. Conf. of the IEEE Engineering in Medicine and Biology Society (IEEE)* 181–4
- [21] Hu X-L, Tong R K, Ho N S, Xue J J, Rong W and Li L S 2015 Wrist rehabilitation assisted by an electromyography-driven neuromuscular electrical stimulation robot after stroke *Neurorehabil. Neural Repair* **29** 767–76
- [22] Colebatch J G, Frackowiak R S J, Brooks D J, Findley L J and Marsden C M 1990 Preliminary report: activation of the cerebellum in essential tremor *Lancet* **336** 1028–30
- [23] Pundik S, McCabe J P, Hrovat K, Fredrickson A E, Tatsuoka C, Feng I J and Daly J J 2015 Recovery of post stroke proximal arm function, driven by complex neuroplastic bilateral brain activation patterns and predicted by baseline motor dysfunction severity *Front. Hum. Neurosci.* **9** 394
- [24] Talelli P, Greenwood R J and Rothwell J C 2006 Arm function after stroke: neurophysiological correlates and recovery mechanisms assessed by transcranial magnetic stimulation *Clin. Neurophysiol.* **117** 1641–59
- [25] Lattari E, Velasques B, Paes F, Cunha M, Budde H, Basile L and Cagy M 2010 Corticomuscular coherence behavior in fine motor control of force: a critical review *Rev. Neurol* **51** 610–23
- [26] Kristeva R, Patino L and Omlor W 2007 Beta-range cortical motor spectral power and corticomuscular coherence as a mechanism for effective corticospinal interaction during steady-state motor output *NeuroImage* **36** 785–92
- [27] Artoni F, Fanciullacci C, Bertolucci F, Panarese A, Makeig S, Micera S and Chisari C 2017 Unidirectional brain to muscle connectivity reveals motor cortex control of leg muscles during stereotyped walking *NeuroImage* **159** 403–16
- [28] Mima T, Matsuoka T and Hallett M 2001 Information flow from the sensorimotor cortex to muscle in humans *Clin. Neurophysiol.* **112** 122–6
- [29] Witham C L, Riddle C N, Baker M R and Baker S N 2011 Contributions of descending and ascending pathways to corticomuscular coherence in humans *J. Physiol.* **589** 3789–800
- [30] Meng F, Tong K-Y, Chan S-T, Wong W-W, Lui K-H, Tang K-W, Gao X and Gao S 2008 Study on connectivity between coherent central rhythm and electromyographic activities *J. Neural Eng.* **5** 324
- [31] Bao S-C, Leung W-C, Cheung V C, Zhou P and Tong K-Y 2019 Pathway-specific modulatory effects of neuromuscular electrical stimulation during pedaling in chronic stroke survivors *J. Neuroeng. Rehabil.* **16** 143
- [32] Gao Y, Ren L, Li R and Zhang Y 2018 Electroencephalogram–electromyography coupling analysis in stroke based on symbolic transfer entropy *Front. Neurol.* **8** 716
- [33] Calautti C, Leroy F, Guinestre J-Y and Baron J-C 2003 Displacement of primary sensorimotor cortex activation after subcortical stroke: a longitudinal PET study with clinical correlation *NeuroImage* **19** 1650–4
- [34] Pineiro R, Pendlebury S, Johansen-Berg H and Matthews P 2001 Functional MRI detects posterior shifts in primary sensorimotor cortex activation after stroke: evidence of local adaptive reorganization? *Stroke* **32** 1134–9
- [35] Mima T, Steger J, Schulman A E, Gerloff C and Hallett M 2000 Electroencephalographic measurement of motor cortex control of muscle activity in humans *Clin. Neurophysiol.* **111** 326–37
- [36] Kong K-H, Chua K S and Lee J 2011 Recovery of upper limb dexterity in patients more than 1 year after stroke: frequency, clinical correlates and predictors *NeuroRehabilitation* **28** 105–11
- [37] Folstein M F, Folstein S E and McHugh P R 1975 ‘Mini-mental state’: a practical method for grading the cognitive state of patients for the clinician *J. Psychiatr. Res.* **12** 189–98
- [38] Fugl-Meyer A R, Jääskö L, Leyman I, Olsson S and Steglind S 1975 The post-stroke hemiplegic patient. 1. A method for evaluation of physical performance *Scand. J. Rehabil. Med.* **7** 13
- [39] Charalambous C P 2014 Interrater reliability of a modified Ashworth scale of muscle spasticity *Classic Papers in Orthopaedics* (Berlin: Springer) pp 415–7
- [40] Mima T, Toma K, Koshy B and Hallett M J S 2001 Coherence between cortical and muscular activities after subcortical stroke *Clin. Neurophysiol.* **32** 2597–601
- [41] Divekar N V and John L R 2013 Neurophysiological, behavioural and perceptual differences between wrist flexion and extension related to sensorimotor monitoring as shown by corticomuscular coherence *Clin. Neurophysiol.* **124** 136–47
- [42] Delorme A and Makeig S 2004 EEGLAB: an open source toolbox for analysis of single-trial EEG dynamics including independent component analysis *J. Neurosci.* **134** 9–21
- [43] Oostenveld R, Fries P, Maris E and Schoffelen J-M 2011 FieldTrip: open source software for advanced analysis of MEG, EEG, and invasive electrophysiological data *Comput. Intell. Neurosci.* **2011** 156869
- [44] Vigário R, Sarela J, Jousmiki V, Hamalainen M and Oja E 2000 Independent component approach to the analysis of EEG and MEG recordings *IEEE Trans. Biomed. Eng.* **47** 589–93
- [45] Shahid S, Sinha R K and Prasad G 2010 Mu and beta rhythm modulations in motor imagery related post-stroke EEG: a study under BCI framework for post-stroke rehabilitation *BMC Neurosci.* **11** 1–2
- [46] Meng F, Tong K-Y, Chan S-T, Wong W-W, Lui K-H, Tang K-W, Gao X and Gao S 2008 Cerebral plasticity after subcortical stroke as revealed by cortico-muscular coherence *IEEE Trans. Neural Syst. Rehabil. Eng.* **17** 234–43
- [47] Geweke J 1982 Measurement of linear dependence and feedback between multiple time series *J. Am. Stat. Assoc.* **77** 304–13
- [48] Delorme A, Mullen T, Kothe C, Akalin Acar Z, Bigdely-Shamlo N, Vankov A and Makeig S 2011 EEGLAB, SIFT, NIFT, BCILAB, and ERICA: new tools for advanced EEG processing *J. Neurosci. Methods* **2011** 10
- [49] Ding M, Bressler S L, Yang W and Liang H J 2000 Short-window spectral analysis of cortical event-related potentials by adaptive multivariate autoregressive modeling: data preprocessing, model validation, and variability assessment *Biol Cybern.* **83** 35–45

- [50] Babiloni F et al 2005 Estimation of the cortical functional connectivity with the multimodal integration of high-resolution EEG and fMRI data by directed transfer function *Neuroimage* **24** 118–31
- [51] Omlor W, Patino L, Hepp-Reymond M-C and Kristeva R 2007 Gamma-range corticomuscular coherence during dynamic force output *NeuroImage* **34** 1191–8
- [52] Lim M, Kim J S, Kim M and Chung C K 2014 Ascending beta oscillation from finger muscle to sensorimotor cortex contributes to enhanced steady-state isometric contraction in humans *Clin. Neurophysiol.* **125** 2036–45
- [53] Johnson A N, Wheaton L A and Shinohara M 2011 Attenuation of corticomuscular coherence with additional motor or non-motor task *Clin. Neurophysiol.* **122** 356–63
- [54] Nowak D A, Grefkes C, Dafotakis M, Küst J, Karbe H and Fink G R 2007 Dexterity is impaired at both hands following unilateral subcortical middle cerebral artery stroke *Eur. J. Neurosci.* **25** 3173–84
- [55] Bowden J L, Taylor J L and McNulty P A 2014 Voluntary activation is reduced in both the more-and less-affected upper limbs after unilateral stroke *Front. Neurol.* **5** 239
- [56] Shingala M C and Rajyaguru A 2015 Comparison of post hoc tests for unequal variance *Int. J. New Technol. Sci. Eng.* **2** 22–33
- [57] Zhou S, Xie P, Chen X, Wang Y, Zhang Y and Du Y 2018 Optimization of relative parameters in transfer entropy estimation and application to corticomuscular coupling in humans *J. Neurosci. Methods* **308** 276–85
- [58] Lackmy-Vallée A, Klomjai W, Bussel B, Katz R and Roche N J 2014 Anodal transcranial direct current stimulation of the motor cortex induces opposite modulation of reciprocal inhibition in wrist extensor and flexor *J. Neurophysiol.* **112** 1505–15
- [59] Glover I S and Baker S N 2020 Corticospinal, and reticulospinal contributions to strength training *J. Neurosci.* **40** 5820–32
- [60] Pennisi G, Alagona G, Rapisarda G, Nicoletti F, Costanzo E, Ferri R, Malaguarnera M and Bella R 2002 Transcranial magnetic stimulation after pure motor stroke *Clin. Neurophysiol.* **113** 1536–43
- [61] McPherson J G, Chen A, Ellis M D, Yao J, Heckman C and Dewald J P A 2018 Progressive recruitment of contralesional cortico-reticulospinal pathways drives motor impairment post stroke *J. Physiol.* **596** 1211–25
- [62] Takeuchi N, Tada T, Chuma T, Matsuo Y and Ikoma K 2007 Disinhibition of the premotor cortex contributes to a maladaptive change in the affected hand after stroke *Stroke* **38** 1551–6
- [63] Frost S, Barbay S, Friel K, Plautz E and Nudo R J 2003 Reorganization of remote cortical regions after ischemic brain injury: a potential substrate for stroke recovery *J. Neurophysiol.* **89** 3205–14
- [64] Ward N S and Cohen L G 2004 Mechanisms underlying recovery of motor function after stroke *Arch. Neurol.* **61** 1844–8
- [65] Baker S N 2007 Oscillatory interactions between sensorimotor cortex and the periphery *Curr. Opin. Neurobiol.* **17** 649–55
- [66] Wang Y, Xie P, Zhou S, Wang X and Yuan Y 2019 Low-intensity pulsed ultrasound modulates multi-frequency band phase synchronization between LFPs and EMG in mice *J. Neural. Eng.* **16** 026036
- [67] Lan Y, Yao J and Dewald J P A 2017 The impact of shoulder abduction loading on volitional hand opening and grasping in chronic hemiparetic stroke *Neurorehabil. Neural Repair* **31** 521–9
- [68] Bartley K, Woodforth I J, Stephen J P H and Burke D 2002 Corticospinal volleys and compound muscle action potentials produced by repetitive transcranial stimulation during spinal surgery *Clin. Neurophysiol.* **113** 78–90
- [69] Stinear C M, Barber P A, Smale P R, Coxon J P, Fleming M K and Byblow W D 2007 Functional potential in chronic stroke patients depends on corticospinal tract integrity *Brain* **130** 170–80
- [70] O'Dwyer N J, Ada L and Neilson P D 1996 Spasticity and muscle contracture following stroke *Brain* **119** 1737–49
- [71] Bertolasi L, Priori A, Tinazzi M, Bertasi V and Rothwell J C 1998 Inhibitory action of forearm flexor muscle afferents on corticospinal outputs to antagonist muscles in humans *J. Physiol.* **511** 947–56
- [72] Udupa K and Chen R 2013 *Central Motor Conduction Time. Handbook of Clinical Neurology* vol 116 (Amsterdam: Elsevier) pp 375–86
- [73] Dum R P and Strick P L 1991 The origin of corticospinal projections from the premotor areas in the frontal lobe *J. Neurosci.* **11** 667–89
- [74] Okabe N, Himi N, Maruyama-Nakamura E, Hayashi N, Narita K and Miyamoto O 2017 Rehabilitative skilled forelimb training enhances axonal remodeling in the corticospinal pathway but not the brainstem-spinal pathways after photothrombotic stroke in the primary motor cortex *PLoS One* **12** e0187413
- [75] Pellegrino L, Coscia M, Pierella C, Giannoni P, Cherif A, Mugnosso M, Marinelli L and Casadio M 2021 Effects of hemispheric stroke localization on the reorganization of arm movements within different mechanical environments *Life* **11** 383
- [76] Schaefer S Y, Haaland K Y and Sainburg R L 2009 Dissociation of initial trajectory and final position errors during visuomotor adaptation following unilateral stroke *Brain Res.* **1298** 78–91
- [77] Lawhern V J, Solon A J, Waytowich N R, Gordon S M, Hung C P and Lance B J 2018 EEGNet: a compact convolutional neural network for EEG-based brain-computer interfaces *J. Neural. Eng.* **15** 056013
- [78] Dodds T A, Martin D P, Stolov W C and Deyo R A 1993 A validation of the functional independence measurement and its performance among rehabilitation inpatients *Arch. Phys. Med. Rehabil.* **74** 531–6
- [79] Yozbatiran N, Der-Yeghiaian L and Cramer S C 2008 A standardized approach to performing the action research arm test *Neurorehabil. Neural Repair* **22** 78–90